17

CONTINUOUS-WAVE OPTICAL PARAMETRIC OSCILLATORS

Majid Ebrahim-Zadeh

ICFO—Institut de Ciencies Fotoniques
Mediterranean Technology Park
Barcelona, Spain, and
Institucio Catalana de Recerca i Estudis Avancats (ICREA)
Passeig Lluis Companys
Barcelona, Spain

17.1 INTRODUCTION

Since the publication of an earlier review on optical parametric oscillators (OPOs) in 2000,[1] there has been remarkable progress in the technological development and applications of OPO devices. Once considered an impractical approach for the generation of coherent radiation, OPOs have now been finally transformed into truly viable, state-of-the-art light sources capable of accessing difficult spectral regions and addressing real applications beyond the reach of conventional lasers. While the first experimental demonstration of an OPO was reported in 1965,[2] for nearly two decades thereafter there was little or no progress in the practical development of OPO devices, owing to the absence of suitable nonlinear materials and laser pump sources. With the advent of a new generation of birefringent nonlinear crystals, most notably β-BaB_2O_4 (BBO), LiB_3O_5 (LBO), and $KTiOPO_4$ (KTP), but also $KTiOAsO_4$ (KTA) and $RbTiOAsO_4$ (RTA) in the mid-1980s, and advances in solid-state laser technology, there began a resurgence of interest in OPOs as potential alternatives to conventional lasers for the generation of coherent radiation in new spectral regions. The high optical damage threshold, moderate optical nonlinearity, and favorable phase-matching properties of the newfound materials led to important breakthroughs in OPO technology. In the years to follow, tremendous progress was achieved in the development of OPO devices, particularly in the pulsed regime, and a variety of OPO systems from the nanosecond to the ultrafast picosecond and femtosecond timescales, and operating from the near-ultraviolet (near-UV) to the infrared (IR) were rapidly developed. These developments led to the availability of a wide range of practical OPO devices and their deployment in new applications, with some systems finding their way to the commercial market. A decade later, in the mid-1990s, the emergence of quasi-phase-matched (QPM) ferroelectric nonlinear crystals, particularly periodically poled $LiNbO_3$ (PPLN) stimulated new impetus for the advancement of continuous-wave (cw) OPO devices, traditionally the most challenging regime for OPO operation due to almost negligible nonlinear gains available under cw pumping. The flexibility offered by grating-engineered QPM materials, allowing access to the highest nonlinear tensor coefficients, combined with noncritical phase matching (NCPM) and long interaction lengths (>50 mm in PPLN), enabled the low available nonlinear gains to be overcome, hence permitting the development of practical cw OPOs in a variety of resonance configurations. As such, the advent of QPM

materials, most notably PPLN, but also periodically poled KTP (PPKTP), $RbTiOAsO_4$ (PPRTA), and $LiTaO_3$ (PPLT), has had an unparalleled impact on cw OPO technology. Combined with advances in novel high-power solid-state crystalline, semiconductor, and fiber pump sources over the past decade, these developments have led to the practical realization of a new class of cw OPOs with previously unattainable performance capabilities with regard to wavelength coverage, output power and efficiency, frequency and power stability, spectral and spatial coherence, and fine frequency tuning.

With their exceptional spectral coverage and tuning versatility, temporal flexibility from the cw to femtosecond timescales, practical performance parameters, and compact solid-state design, OPO devices have now been firmly established as truly competitive alternatives to conventional lasers and other technologies for the generation of widely tunable coherent radiation in difficult spectral and temporal domains. In the current state of technology, OPO devices can provide spectral access from ~400 nm in the ultraviolet (UV) to ~12 μm in the mid-infrared (mid-IR), as well as the terahertz (THz) spectral region. They can also provide temporal output from the cw and long-pulse microsecond regime to nanosecond, picosecond, and ultrafast sub-20 fs timescales. Many of the developed OPO systems are now routinely deployed in a variety of applications including spectroscopy, optical microscopy, environmental trace gas detection and monitoring, life sciences, biomedicine, optical frequency metrology and synthesis, and imaging.

The aim of this chapter is to provide an overview of the advances in OPO device technology and applications since the publication of the earlier review in 2000.[1] The chapter is concerned only with the developments after 2000, since many of the important advances in this area prior to that date can already be found in the previous treatment[1] as well as other reviews on the subject.[3–10] Because of limited scope, and given that most of the important advances over the last decade have been in the CW operating regime, the chapter is focused only on a discussion of cw OPOs. Reviews on pulsed and ultrafast OPOs can be found elsewhere.[3,4,6–10] This chapter also does not include a description of the fundamental concepts in nonlinear and crystal optics, parametric generation, amplification and gain, or a comprehensive description of the design criteria and operating principles of OPO devices, which have been the subject of several earlier treatments.[11–16]

17.2 CONTINUOUS-WAVE OPTICAL PARAMETRIC OSCILLATORS

Of the different types of OPO devices developed to date, advancement of practical OPOs in the cw operating regime has been traditionally most difficult, since the substantially lower nonlinear gains available under cw pumping necessitate the use of high-power cw pump laser or the deployment of multiple-resonant cavities to reach operation threshold. As in a conventional laser oscillator, the OPO is characterised by a threshold condition, defined by the pumping intensity at which the growth of the parametric waves in one round-trip of the optical cavity just balances the total loss in that round-trip. Once threshold has been surpassed, coherent light at macroscopic levels can be extracted from the oscillator. In order to provide feedback in an OPO, a variety of resonance schemes may be deployed by suitable choice of mirrors forming the optical cavity, as illustrated in Fig. 1*a* to *e*. The mirrors may be highly reflecting at only one of the parametric waves (*signal* or *idler*, but not both), as in Fig. 1*a*, in which case the device is known as a *singly resonant oscillator* (SRO). This configuration is characterised by the highest cw operation threshold. In order to reduce threshold, alternative resonator schemes may be employed where additional optical waves are resonated in the optical cavity. These include the *doubly resonant oscillator* (DRO), Fig. 1*b*, in which both the signal and idler waves are resonant in the optical cavity, and the *pump-resonant* or *pump-enhanced* SRO, Fig. 1*c*, where the *pump* as well as one of the generated waves (signal or idler) is resonated. In an alternative scheme, Fig. 1*d*, the pump may be resonated together with both parametric waves, in which case the device is known as a *triply resonant oscillator* (TRO). Such schemes can bring about substantial reductions in threshold from the cw SRO configuration, with the TRO offering the lowest operation threshold. In an alternative scheme, the external pump power threshold for a cw SRO may also be substantially reduced by deploying internal pumping, where the OPO is placed inside

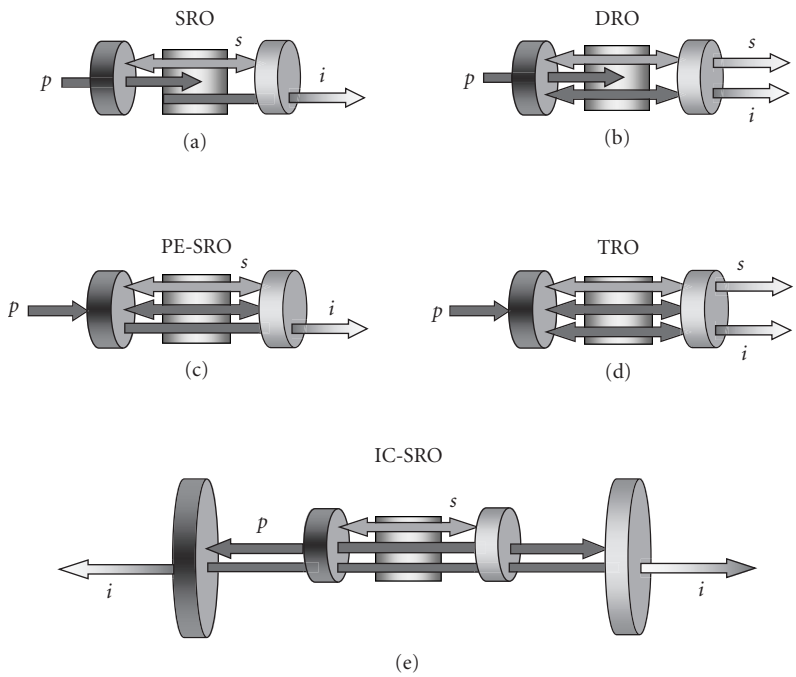

FIGURE 1 Cavity resonance configurations for cw OPOs. The symbols *p*, *s*, and *i* denote *pump, signal*, and *idler*, repectively.

a minimally output-coupled pump laser. A schematic of such an *intracavity SRO* (*IC-SRO*) is illustrated in Fig. 1*e*.

The comparison of steady-state threshold for conventional externally pumped cw OPOs under different resonance schemes is shown in Fig. 2, where the calculated external pump power threshold is plotted as a function of the effective nonlinear coefficient of several materials including LBO, KTA, KTP, $KNbO_3$, PPLN, and PPRTA. From the plot, it is clear that for the majority of birefringent materials the attainment of cw SRO threshold requires pump powers on the order of tens of watts, well outside the range of the most widely available cw laser sources. However, in the case of PPLN, the cw SRO threshold is substantially reduced to acceptable levels below ~1 W, bringing operation of cw SROs within the convenient range of widespread cw solid-state pump lasers. With the cw PE-SRO, considerably lower thresholds can be achieved, from a few hundred milliwatts to ~1 W for birefringent materials and below ~100 mW for PPLN. In the case of cw DRO, still lower thresholds of the order of 100 mW are attainable with birefringent materials, with only a few milliwatts for PPLN, whereas with the cw TRO, thresholds from below 1 mW to a few milliwatts can be obtained in birefringent materials.

It is thus clear that practical operation of cw OPOs in SRO configurations is generally beyond the reach of birefringent materials, but requires DRO, TRO, and PE-SRO cavities. On the other hand, implementation of cw SROs necessitates the use of PPLN or similar QPM materials, offering enhanced optical nonlinearities, and long interaction lengths under NCPM. However, the threshold reduction from SRO to PE-SRO, DRO, and TRO cavity configurations is often achieved at the expense of increased spectral and power instability in the OPO output arising from the difficulty in maintaining resonance for more than one optical wave in a single optical cavity. For this reason, the cw SRO offers the most direct route to the attainment of high output stability and spectral control without stringent demands on the frequency stability of the laser pump source. On the other hand,

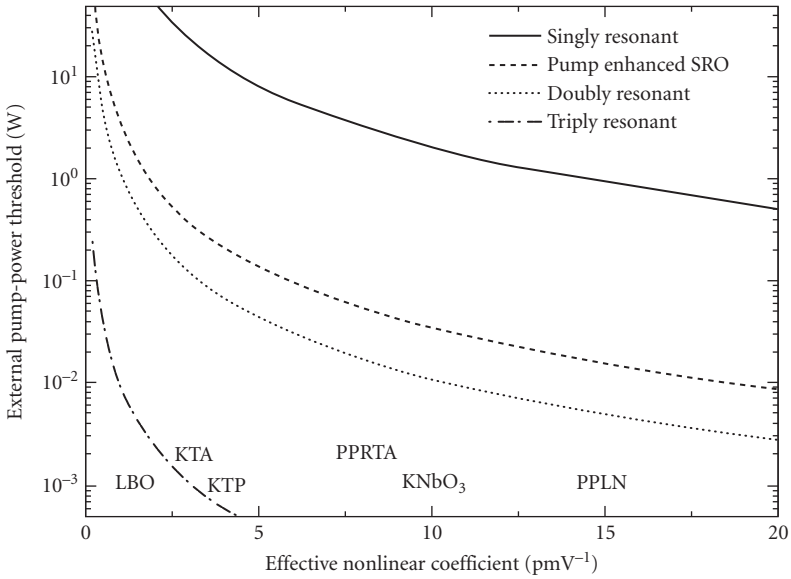

FIGURE 2 Calculated minimum thresholds for different OPO resonance configurations versus the effective nonlinear coefficients in various nonlinear materials. The calculation assumes confocal focusing and loss values that are typically encountered in experimental cw OPOs, the finesses representing round-trip power losses of approximately 2.0 percent. The plots correspond to a pump wavelength of 800 nm, degenerate operation, a pump refractive index of ~1.7, a crystal length of 20 mm, signal and idler cavity finesses of ~300, and a pump enhancement factor of ~30. In the case of PE-SRO and TRO, the enhancement factor of 30 represents the maximum enhancement attainable with parasitic losses of ~3 percent at the pump.[17]

practical implementation of cw PE-SRO, DRO, and TRO requires active stabilization techniques to control output power and frequency stability, with the PE-SRO offering the most robust configuration for active stabilization and TRO representing the most difficult in practice. In addition, practical operation of OPOs in multiple resonant cavities can only be achieved using stable, single-frequency pump lasers and such devices also require more complex protocols for frequency tuning and control than the cw SRO. More detailed description of the different resonance and pumping schemes for OPOs and analytical treatment of tuning mechanisms, spectral behavior, frequency control, and stabilisation can be found in an earlier review.[1]

Singly Resonant Oscillators

By deploying the intracavity pumping scheme using a Ti:sapphire laser in combination with a 20-mm PPKTP crystal, Edwards et al.[18] reported a cw IC-SRO capable of providing up to 455 mW of non-resonant infrared idler power at a down-conversion efficiency of 87 percent. Using a combination of pump tuning at room temperature and crystal temperature tuning, idler (signal) coverage in the 2.23 to 2.73 μm (1.14 to 1.27 μm) spectral ranges was demonstrated. By configuring the Ti:sapphire pump laser and the SRO in ring cavity geometries and using intracavity etalons, 115 mW of unidirectional, single-frequency idler power was generated at 2.35 μm with mode-hop-free operating time intervals of about 10 s under free-running conditions. The resonant signal was measured to have a linewidth <15 MHz for a pump linewidth <25 MHz.

The advent of PPLN with large effective nonlinearity (d_{eff} ~15 pm/V) and long interaction lengths (currently up to 80 mm) under NCPM has enabled the development of cw SROs in conventional

external pumping configurations using more commonly available, moderate- to high-power solid-date pump sources. By deploying a fixed-frequency, cw, single-mode Nd:YVO_4 pump laser at 1.064 μm, Bisson et al.[19] developed a portable source for mid-IR photoacoustic spectroscopy based on a PPLN cw SRO by using discrete mode-hop tuning of the idler. The SRO, based on a 50-mm PPLN crystal with fanned grating (Λ = 29.3 to 30.1 μm), was configured in a ring cavity, and frequency selection and fine tuning was implemented using solid or air-spaced intracavity etalons. With an uncoated, 400-μm-thick, solid Nd:YAG etalon, a total mode-hop-tuning range of ~4 cm^{-1} for the idler in discrete steps of 0.02 to 0.1 cm^{-1} was achieved by rotation of the etalon. The SRO could deliver a maximum idler power of ~120 mW at a pump depletion of 40 to 50 percent for 6 W of pump power. Using the mode-hop-tuned idler output near 3.3 μm, photoacoustic spectroscopy of the methane Q branch was performed at atmospheric pressure by simultaneous tuning of the PPLN crystal combined with etalon rotation. A total of four etalon scans covering ~10 cm^{-1} was necessary to trace the Q branch spectrum. In an effort to achieve a constant tuning rate as well as minimize insertion loss due to etalon rotation, which in turn leads to mode hops arising from variable heating of the PPLN crystal due to the changes in intracavity power, an alternative air-spaced fused silica etalon with ~0.5 to 1.5 mm spacing and ~5 percent reflectivity at the signal (~1.57 μm) was also employed in the present device. While resulting in a higher oscillation threshold (~4 W) and lower idler output (~80 mW), the combination of PPLN tuning and piezoelectric scan of the etalon over a distance of 3 μm (at 1.5 mm separation) yielded a total mode-hop tuning range of ~14 cm^{-1} for the idler at a constant tuning rate and in discrete steps of 0.1 cm^{-1}, providing sufficient resolution for atmospheric sensing and pressure-broadened spectroscopy. The measured linewidth of the idler was <10 MHz with a passive stability of ~50 MHz over 30 s.

By using a 10-W cw single-frequency diode-pumped Nd:YAG laser at 1.064 μm, Van Herpen et al.[20] demonstrated a cw SRO based on PPLN with a mid-IR idler tuning range of 3.0 to 3.8 μm. The SRO, configured in a ring cavity and using a crystal with fanned grating (L = 50 mm, Λ = 29.3 to 30.1 μm) exhibited a pump power threshold of ~3 W and could provide a maximum idler output power of 1.5 W at 3.3 μm for 9 W of pump power. The combination of the single-mode pump laser, a ring cavity for the SRO, and the inclusion of an intracavity air-spaced etalon enabled mode-hop-free tuning of the idler over 12 GHz by tuning the pump frequency over 24 GHz, with the idler mode-hop tuning range limited by mode hopping in the pump laser. Under this condition, 700 mW of single-frequency, smoothly tunable idler power could be provided by the SRO. In a later experiment,[21] using the same PPLN crystal and identical cavity design for the SRO, the authors were able to improve the idler output power in the 3.0 to 3.8 μm range by increasing the available Nd:YAG pump power to 15 W and by optimizing pump focusing and the SRO cavity length. The SRO similarly exhibited a cw power threshold of ~3 W, but could provide 2.2 W of idler power for 10.5 W of input pump power. The coarse and fine tuning properties of this SRO were similar to the earlier device. For fine tuning, an intracavity air-spaced etalon with variable spacing of 0.2 to 3 mm (FSR = 50 to 750 GHz) was used. Continuous scanning of etalon spacing resulted in discrete mode-hop tuning of the idler over 100 GHz. With a 400-μm uncoated solid YAG etalon (FSR = 207 GHz), an idler mode-hop tuning range of 10 cm^{-1} in steps of 0.02 to 0.1 cm^{-1} (0.6 to 3 GHz) could be obtained by rotation of the etalon. Subsequently, using the same pump laser, the authors reported a cw SRO based on a multigrating PPLN crystal (Λ = 25.9 to 28.7 μm) and providing extended idler coverage into the 3.7 to 4.7 μm spectral range in the mid-IR.[22] The ring-cavity SRO exhibited an oscillation threshold of between 5 and 7.5 W over this spectral range and for an input pump power of 11 W could provide a maximum idler output of 1.2 W at 3.9 μm, decreasing to 120 mW at 4.7 μm. The increase in SRO threshold and corresponding decrease in output power were attributed to the increasing idler absorption in PPLN at longer wavelengths toward 5 μm. With the inclusion of the same 400-μm uncoated YAG etalon to stabilize the resonant signal frequency, continuous mode-hop free tuning of the idler was achieved by tuning the pump frequency over 24 GHz, but with a reduction in idler power by as much as 50 percent. Discontinuous mode-hop tuning of the idler output could also be obtained through rotation of the intracavity etalon. In a later report, the use of a tunable high-power (>20 W) diode-pumped Yb:YAG laser in combination with two PPLN crystals with fanned gratings (Λ = 28.5 to 29.9 μm) and two sets of OPO mirrors enabled the generation of widely tunable idler radiation with a total tuning range of 2.6 to 4.66 μm, and at increased

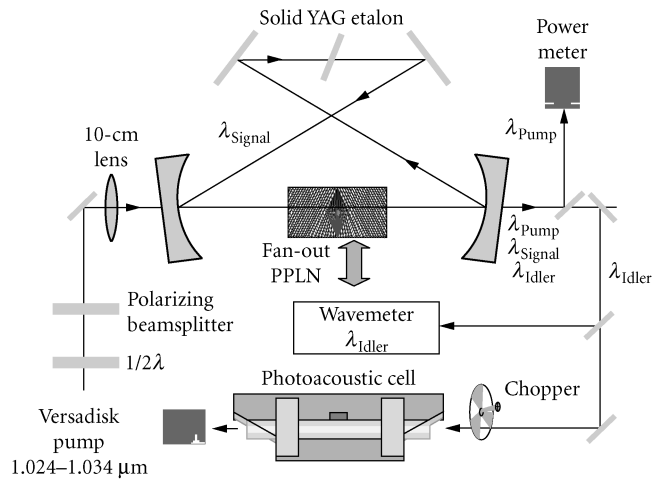

FIGURE 3 Experimental setup of the cw SRO. The pump wavelength varies from 1024 to 1034 nm and the idler wavelength from 2.6 to 4.7 μm. A pump rejecter mirror separates the pump light from the idler and signal beams, after which the idler beam is reflected toward the wavemeter and photoacoustic cell. The signal wavelength can be measured with the same wavemeter by replacing the idler reflector with a signal reflector.[23]

cw power levels up to 3 W.[23] For frequency stability, a 400-μm uncoated YAG etalon (FSR = 207 GHz) was similarly used internal to the SRO cavity (Fig. 3). The SRO had a threshold of 8 W and, with nonoptimized mirror and crystal coatings, could provide 3.0 W of mid-IR idler output at 2.954 μm for 18 W of pump power. The SRO could provide an idler mode-hop tuning range of 25 GHz in steps of 100 MHz (FSR of the pump laser cavity) by tuning the intracavity pump etalon. Combined with the tuning of the Lyot filter within the pump laser, a total mode-hop tuning range of 190 GHz could be scanned, limited by a mode hop in signal frequency of 207 GHz corresponding to the FSR of the YAG etalon within the SRO cavity. By recording the photoacoustic signal in ethane, the authors characterized the frequency stability of the SRO. Due to unoptimized coatings, the idler exhibited frequency instabilities of 90 MHz/s, while temperature fluctuations in the PPLN crystal resulted in an idler frequency drift of 250 MHz over 200 s. In the same report, the authors demonstrated extension of the idler wavelength to 3.3 to 4.66 μm using the broad tuning of the pump laser (1.024 to 1.034 μm) in combination with grating tuning of the PPLN crystal, providing 200 mW of idler power at 4.235 μm, corresponding to the strongest CO_2 absorption line.

Subsequently, Ngai et al.[24] reported a cw SRO with automatic tuning control based on a multigrating MgO:PPLN (L = 50 mm, Λ = 29.0 to 31.5 μm). A schematic of the experimental setup is shown in Fig. 4. The SRO was pumped by a master oscillator-power amplifier (MOPA) laser at 1064 nm, providing 11.5 W of single-frequency output with a linewidth of 5 kHz (over 1 ms), frequency stability of 50 MHz/h, and continuous tuning over 48 GHz. The combination of temperature and grating tuning in the MgO:PPLN crystal provided coarse coverage over 2.75 to 3.83 μm in the idler and 1.47 to 1.73 μm in the signal, with a maximum idler power of 2.75 W. By using a ring SRO cavity containing a 400-μm-thick uncoated solid YAG etalon (FSR = 207 GHz), a short-term frequency stability of 4.5 MHz over 1 s was attainable in the absence of active stabilization. Fine wavelength scanning of the idler output was achieved through a combination of pump tuning, etalon rotation, and temperature tuning using an automated process with computer control. First, by continuous tuning of the pump frequency over 48 GHz at a fixed etalon angle, the idler could be tuned over 12 GHz before the occurrence of a mode hop in the pump laser (Fig. 5). The total idler tuning range attainable in this way was 207 GHz, limited by an etalon mode hop. Then, by rotation of the

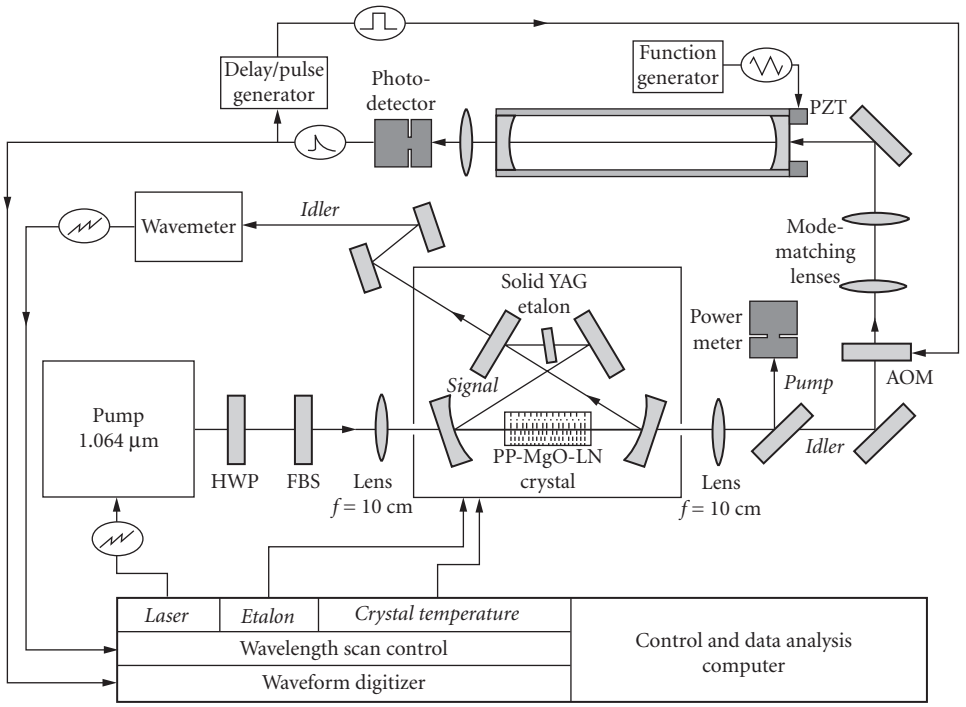

FIGURE 4 Experimental setup of automatically tunable cw SRO combined with continuous-wave cavity leak-out spectroscopy. The OPO cavity is resonant for the signal wavelength. The idler beam is sent to a cw leak-out cavity and to a wavemeter.[24]

etalon to a new angle, the pump was again scanned until a new total tuning range of 207 GHz was covered, and process was repeated. Finally, changing the crystal temperature by 2 to 5°C, and repeating the entire process, wavelength scans of up to 450 cm^{-1} with a resolution of $<5 \times 10^{-4}$ cm^{-1} could be obtained with a single grating period. Using this automated tuning process, the utility of the cw SRO for sensitive detection of CO_2, methane, and ethane was demonstrated with photoacoustic and cavity leak-out spectroscopy, and analysis of human breath was performed by recording the absorption spectra of methane, ethane, and water in two test persons using photoacoustic spectroscopy.

With the continued advances in pump laser technology, the development of cw SROs based on high-power diode-pumped fiber lasers and amplifiers has also become a reality. Fiber lasers are attractive alternatives as pump sources for cw SROs, because they combine the high-power properties of crystalline solid-state laser materials with significant wavelength tuning and excellent spatial beam quality in compact and portable design. The pump tuning capability allows rapid and wide tuning of the SRO output without recourse to temperature or grating period variation, while the high available powers and excellent beam quality allow access to SRO threshold and enable the generation of practical output powers. The use of fiber pump lasers can thus provide a versatile class of cw SROs for the mid-IR that offer the advantages of simplicity, compact all-solid-state design, portability, reduced cost, improved functionality, and high output power and efficiency. Operation of a cw SRO pumped by a fiber laser was first reported by Gross et al.[25] using a tunable Yb-doped fiber laser. The laser delivered more than 8 W of cw output power in excellent spatial beam quality and was tunable over the wavelength range of 1031 to 1100 nm. With the use of a 40-mm-long multigrating PPLN crystal and a ring cavity for the SRO, a cw idler output power of 1.9 W was generated at a wavelength of 3.2 μm in the mid-IR for 8.3 W of fiber pump power, with a corresponding SRO power threshold of 3.5 W. Idler wavelength tuning over 3.057 to 3.574 μm could be accomplished

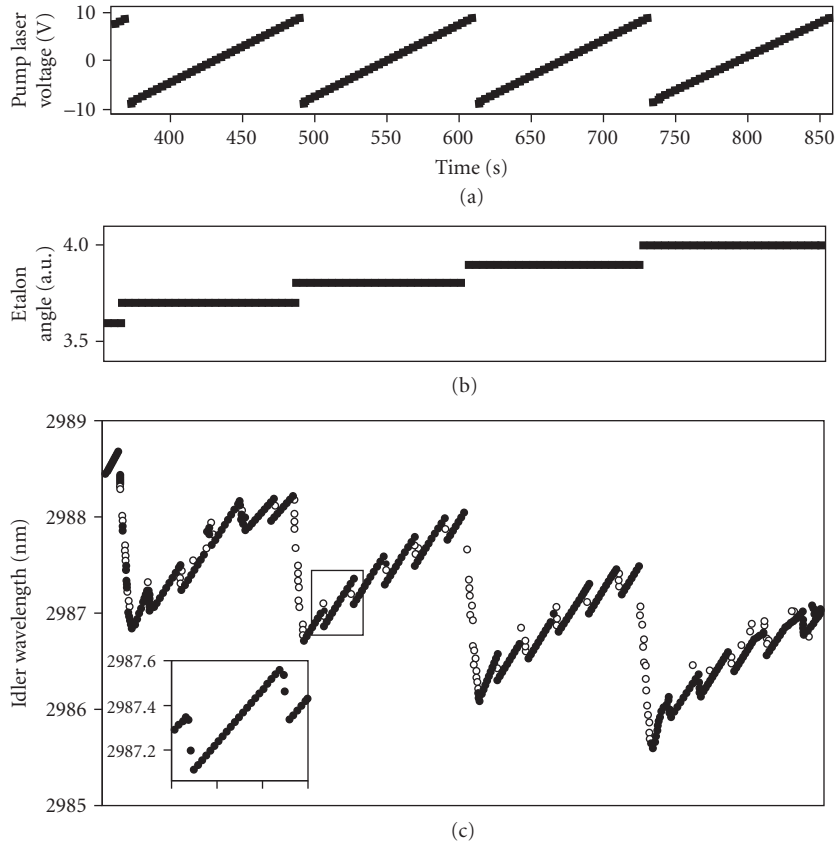

FIGURE 5 Combined pump-etalon scan. By scanning the pump laser (*a*) and stepping the etalon angle after each pump laser scan (*b*), a continuous wavelength coverage over 207 GHz can be realized (*c*). The resolution of the idler frequency is limited by the resolution of the wavemeter [*inset* in (*c*)].[24]

by varying the crystal temperature or changing the grating period. However, wider and more convenient wavelength tuning was also available by exploiting the tuning capability of the fiber pump laser, where an idler tuning range of more than 700 nm over 2.980 to 3.700 μm was obtained by varying the pump wavelength between 1.032 and 1.095 μm. In a subsequent experiment, Klein et al.[26] demonstrated rapid wavelength tuning of a similar cw SRO by using electronic wavelength control of the Yb-doped fiber pump laser with an acousto-optic tunable filter. The SRO, based on a 40-mm-long single-grating PPLN crystal, was arranged in a similar ring cavity and, at a fixed crystal temperature and grating period, could be rapidly tuned over 3.160 to 3.500 μm in the idler wavelength by electronically tuning the fiber pump laser from 1060 to 1094 nm. The 340-nm idler tuning could be achieved within a time interval of 330 μs, representing a frequency tuning rate of 28 THz/ms. The overall electronic tuning range of the fiber pump laser over 1.057 to 1.100 μm resulted in an SRO idler tuning range of 437 nm in the mid-IR, from 3.132 to 3.569 μm. For the maximum fiber pump power of 6.6 W at 1.074 μm, the SRO generated an idler output power of 1.13 W at 3.200 μm.

More recently, operation of a low-threshold mid-IR cw SRO was reported by Henderson and Stafford[27] using MgO:PPLN and an all-fiber laser pump source. A schematic of the experimental setup is shown in Fig. 6. The cw single-frequency pump at 1083 nm was configured in a MOPA

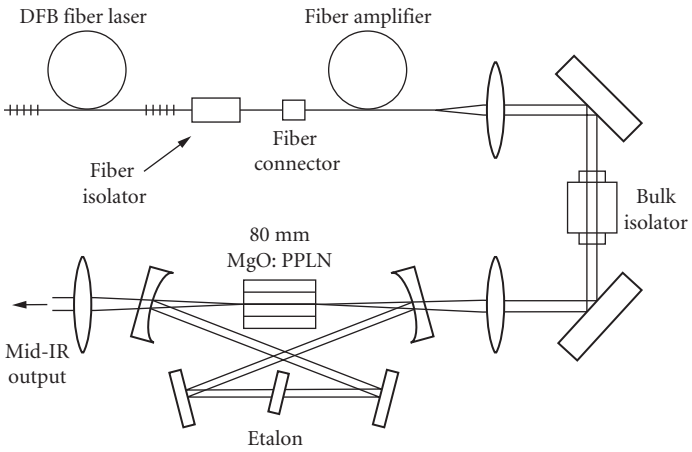

FIGURE 6 Schematic of experimental configuration for the fiber-pumped cw SRO.[27]

arrangement using a 20-mW distributed feedback (DFB) fiber laser with 50-kHz linewidth as the seed and a polarization-maintaining fiber as the amplifier. The use of fiber connection between the two stages ensured an all-fiber configuration with no free-space components, alignment-free injection, and minimum long-term cavity misalignment. The MOPA could provide up to 3.5 W of amplified single-mode pump power for 20 mW of input seed power. Using multigrating and fanned crystals (Λ = 31.3 to 32.5 μm) of 80-mm interaction length and operating the SRO just above room temperature (30°C), oscillation thresholds as low as 780 mW were obtained, with up to 750 mW of idler power generated for 2.8 W of fiber pump power. The idler output was tunable over 2650 to 3200 nm with a near-diffraction-limited spatial mode up to 500 mW and beam quality factor $M^2 = 1.04$. By exploiting the tunability of the pump laser through application of a voltage to the piezoelectric transducer attached to the fiber (rapid) and temperature variation of the seed source (slow), continuous mode-hop-free tuning of the idler over more than 120 GHz was demonstrated (Fig. 7). Using a Fabry-Perot interferometer, the idler linewidth was measured to be 1.1 MHz at 3.17 μm. The narrow linewidth, broad coarse wavelength coverage, and rapid mode-hop-free tuning of the idler through piezoelectric tuning of the pump enabled high-resolution spectroscopy in a variety of mid-IR gases including water vapor, CO_2, and methane.

The development of PPLN has also led to substantial reductions in cw SRO power threshold, compatible with the direct use of semiconductor diode lasers as pumps for cw SROs. In addition to a compact design, an important advantage of this approach is the tunability of diode laser, which allows rapid and continuous tuning of SRO output at a fixed temperature and grating period through pump tuning. However, to provide the sufficiently high cw pump powers (typically >1 W) and the highest beam quality to attain SRO threshold, it has been necessary to boost the available power from single-mode diode lasers using amplification schemes. By employing a grating stabilized, extended-cavity single-stripe InGaAs semiconductor diode laser at 924 nm as a master oscillator and a single-pass tapered amplifier, Klein et al.[28] demonstrated operation of a cw SRO based on a 38-mm-long PPLN crystal with a pump power threshold of 1.9 W. For 2.25 W of diode pump power, 200 mW of single-frequency idler radiation was generated at 2.11 μm. Wavelength tuning was achieved by electronic control of the master oscillator cavity, providing continuous mode-hop-free tuning of the diode pump radiation over 60 GHz from the power amplifier with a corresponding linewidth of <4 MHz. By using an intracavity etalon to fix the resonant signal frequency, a continuous mode-hop-free idler tuning of 56 GHz was obtained at 2.11 μm by tuning the pump wavelength. In an alternative scheme, using a distributed Bragg reflector (DBR) diode laser at 1082 nm, which was amplified in an Yb-doped fiber, Lindsay et al.[29] achieved rapid mode-hop-free tuning of a mid-IR cw SRO. A schematic of the experimental configuration is shown in Fig. 8, and the SRO idler

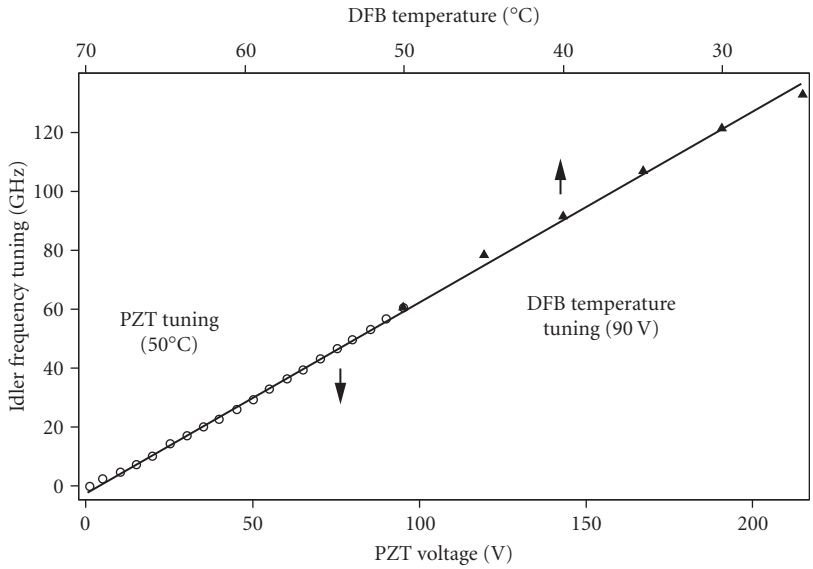

FIGURE 7 Fine tuning of the OPO idler frequency measured as a function of pump tuning parameter, performed by PZT voltage and fiber temperature variation.[27]

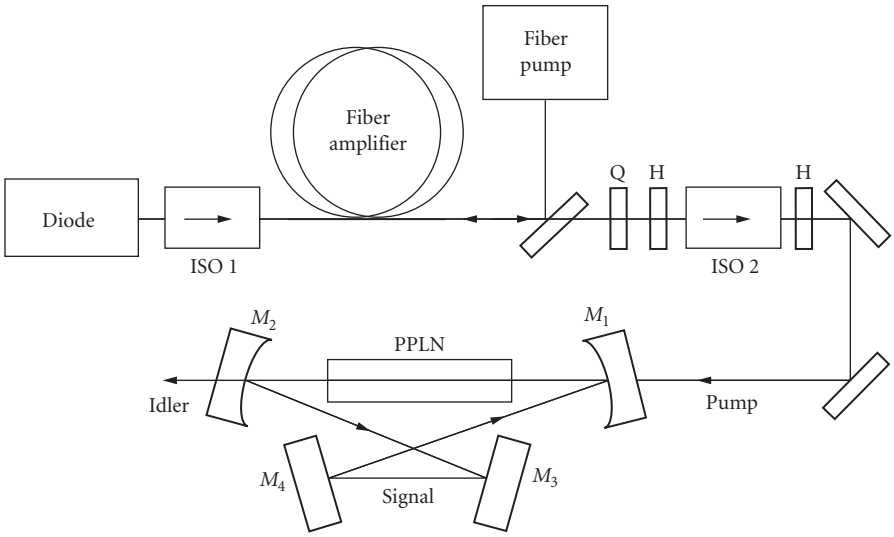

FIGURE 8 Schematic of experimental arrangement for the cw SRO pumped by a fiber-amplified DBR diode laser.[29]

output power and tuning range are shown in Fig. 9. The SRO was based on a 40-mm PPLN crystal and could provide rapid continuous tuning over 110 GHz in 29 ms. Coarse and discontinuous wavelength tuning of the idler wave was also obtained over 20 nm by tuning the DBR diode laser, and more than 1 W of idler output power was generated across the 3.405 to 3425 μm range for 6.9 W of input pump power. An overall idler tuning range of 300 nm in the 3 to 3.5 μm band in the mid-IR was also available by varying the temperature of the PPLN crystal.

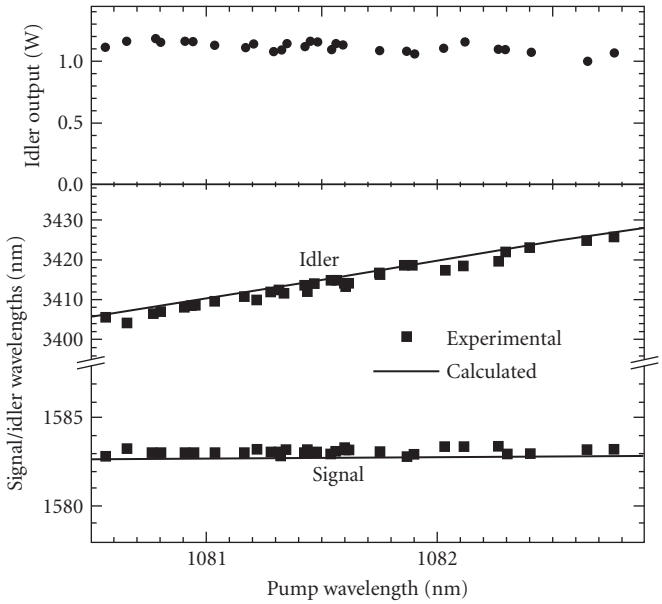

FIGURE 9 Variation of OPO output wavelengths (lower plot), and corresponding idler output power (upper plot), during pump tuning by seed laser DBR section alone. PPLN grating period was 29.75 μm and temperature was 180.5°C. Solid lines are calculated tuning range.[29]

The availability of increasingly powerful pump sources such as cw fiber lasers, together with the high nonlinear coefficient (d_{eff} ~17 pm/V) and long interaction lengths (50 to 80 mm) in PPLN, can now readily permit practical operation of cw SROs many times above operation threshold, providing multiwatt idler output powers. At the same time, the presence of high optical powers can lead to additional linear and nonlinear optical effects which can modify SRO output characteristics. These include thermal loading of the crystal due to linear absorption, which can result in thermal lensing, thermal phase mismatching and output beam quality degradation, or spectral generation and broadening due to higher-order nonlinear optical effects. As such, optimum performance of cw SROs at high pump powers requires strategies to combat such effects in order to achieve maximum conversion efficiency and output extraction at full pump power, while maintaining the highest spectral and spatial beam quality, power, and frequency stability. The performance characteristics of cw SROs at high pump powers many times threshold have been studied by Henderson and Stafford.[30] By deploying a 15-W cw single-frequency Yb fiber laser at 1064 nm as the pump and 50-mm MgO:PPLN crystals with multiple (Λ = 31.5 to 32.1 μm) and fanned (Λ = 30.8 to 31.65 μm) gratings, they investigated the effects of pump power on crystal heating, wavelength tuning, beam quality, and optimum output power and extraction efficiency. With the high beam quality of the fiber laser (M^2 ~ 1.06), and using a ring cavity with mirrors of highest reflectivity at the signal (R ~ 99.9 percent) and optimum mode-matching, they achieved a threshold as low as 1.0 W, enabling SRO operation at up to 15 times threshold. With the multigrating crystal, the SRO reached a pump depletion of 91 percent at 2.5 times threshold, remaining constant to within ~10 percent up to the maximum pump power at 15 times above threshold. The idler output, measured at 2610 nm, exhibited a linear increase with input pump power, reaching 4.5 W at 15 W of pump, with a corresponding external photon conversion efficiency of ~74 percent. However, operation of SRO at increasing levels of pump power was found to result in a passive increase in crystal temperature and thus a shift in the output wavelength. At the highest pump power the rise in crystal temperature was as much as 23°C, leading to a significant shift in

signal (26 nm) and idler (57 nm) wavelengths compared to operation at low pump power. Given the minimal absorption of the MgO:PPLN crystal at idler wavelengths of 2 to 3 μm in this SRO, the self-heating effect was attributed to the finite absorption of the intracavity signal power. To confirm this, the authors deployed output coupling of the signal by replacing one of the high reflectors with a 4.2 percent output coupler. By operating the SRO at an ambient temperature of 26°C, they observed a 22°C rise in crystal temperature to 47°C under minimum output coupling at the maximum pump power. However, when using the 4.2 percent output coupler, the corresponding temperature rise was only 2.5°C, from 26°C to 28.5°C. Using measurements of signal output power, they estimated the circulating signal power to be as high as ~1.4 kW at the maximum pump power under minimum output coupling, decreasing to ~100 W with the 4.2 percent output coupler. By estimating the total absorption in the 50-mm crystal as 0.4 percent (0.08 percent/cm), they were able to conclude that an absorbed signal power of 5 W was responsible for the 22°C rise in crystal temperature. These measurements clearly confirmed the role of the intracavity signal power in heating of the MgO:PPLN crystal and its influence on spectral shifting of SRO output. The rise in crystal temperature was also observed to have a significant influence on the degradation of spatial quality of the idler beam by inducing thermal lensing effects within the crystal. From measurement of idler beam quality at the same output power level of 3.2 W, they were able to deduce a quality factor of $M^2 \sim 1.35$ under minimum output coupling compared to $M^2 \sim 1.0$ when using the 4.2 percent output coupler, hence confirming the deleterious effects of high circulating signal power on SRO beam quality and thus the need for optimization of output coupling at a given pump power to achieve the highest beam quality while maintaining maximum extraction efficiency. To this end, the authors also investigated the optimization of SRO output power and extraction efficiency at the maximum pump power by using variable output coupling (0 to 5 percent) for the signal across a limited tuning range. Using the fanned crystal, they found the optimum output coupling value to be 3.0 percent, resulting in the simultaneous extraction of 3.0 W of idler and 4.2 W of signal at an overall extraction efficiency of 48 percent. Under this condition, the pump depletion was 78 percent and SRO threshold was 5.8 W, corresponding to the optimum pumping ratio of ~2.5 for maximum power extraction. The effect of use of signal output coupling as a means of optimizing the performance of cw SROs was also later investigated in a separate experiment by Samanta and Ebrahim-Zadeh.[31] Using a cw SRO based on MgO:sPPLT pumped at 532 nm, the authors demonstrated improvements of 1.08 W in total output power, 10 percent in total extraction efficiency, and a 130-nm extension in the useful tuning range, while maintaining pump depletions of 70 percent, idler output powers of 2.59 W, and a minimal increase in oscillation threshold of 24 percent. The output-coupled cw SRO could deliver a total power of up to 3.6 W at 40 percent extraction efficiency across 848 to 1427 nm. The single-frequency resonant signal also exhibited a higher spectral purity than the nonresonant idler output.

The high nonlinear gain coefficient of PPLN combined with the large optical powers present in cw SROs has also been observed to give rise to higher-order nonlinear effects in addition to the second-order parametric process. In a recent example of such an effect,[32] operation of a cw SRO based on MgO:PPLN was reported together with simultaneous Raman action driven by the high intracavity signal intensity. The SRO, based on a multigrating MgO:PPLN crystal (L = 50 mm, Λ = 28.5 to 31.5 μm), was configured in a linear standing-wave cavity and pumped by a 10-W Yb fiber laser at 1070 nm. Two sets of cavity mirrors were used for the SRO, providing different reflectivities for the signal over 1500 to 1700 nm. With the low-Q cavity (R = 98.2 to 99 percent; Q ~ 10^8), normal cw SRO operation with the expected signal and idler spectra was achieved with a 3.3-W threshold, and 1.6 W of idler power was generated at 3620 nm for 8 W of pump at an optical efficiency of 20 percent and slope efficiency of 35 percent. With the high-Q SRO cavity (R = 99.4 to 99.8 percent; Q ~ 10^9), stimulated Raman action with characteristic spectra was simultaneously observed in the vicinity of signal spectrum, driven by the tenfold increase in intracavity signal power to ~100 W. The cw SRO threshold in this case was reduced to 0.5 W, with a corresponding reduction in optical efficiency to 16 percent and slope efficiency to 15 percent. The pump power threshold for Raman conversion was 1.9 W. While stimulated by intracavity signal power, Raman action was present only for grating periods and mirror reflectivities with lowest loss at the corresponding wavelengths, confirming the resonant nature of the observed effect. It was also observed that the presence of Raman oscillation with the high-Q SRO cavity resulted in improved idler RMS power stability of 1.46 percent compared to a 4.1 percent variation with the low-Q cavity, suggesting power limiting of intracavity signal by the Raman conversion.

In a subsequent experiment, Henderson and Stafford[33] also observed stimulated Raman oscillation in a high-power cw SRO based on MgO:PPLN. Using a 14.5-W cw single-frequency Yb fiber laser at 1064 nm and the same SRO arrangement as in Ref. 30, they observed Raman conversion of the intracavity signal under minimum output coupling and at pump powers more than 2 times above threshold, corresponding to circulating signal powers in excess of 230 W. Because of the increasing loss of SRO cavity across an extended tuning range, only two components of the Raman spectrum could be observed. However, under conditions of output coupling no Raman generation was observed up to the maximum available pump corresponding to 170 W of intracavity signal power. In the same cw SRO, the authors also observed spectral broadening of the resonant signal wave at high pump powers. Using highly reflecting mirrors to minimize threshold to 1.5 W, they were able to investigate the evolution of signal spectrum with pump power above threshold. It was observed that while at pump powers up to 3 times above threshold, the signal spectrum remained single-frequency, at pumping ratios between 3 to 4.7 the spectrum exhibited broadening with a symmetric pattern of side modes. The side modes were separated by between 0.2 and 0.5 nm, with their number and intensity increasing with pump power. Above a pumping ratio of 4.7, the signal spectrum was observed to become continuous with a FWHM bandwidth of ~2 nm. These observations, which were found to be in qualitative agreement with predicted theory, confirm that the operation of cw SROs at high pump powers and under the conditions of minimum signal coupling must be limited below a critical pumping ratio of ~4.5, if single-frequency oscillation is to be maintained. Since the maximum conversion in the same experiments was found to be attainable at a pumping ratio of 2.5, by choosing an optimum output coupling of 3.0 percent, the authors increased the SRO threshold to 5.1 W and so were able to maintain single-frequency operation up to the full available pump power of 14.5 W by remaining above the optimum pumping ratio (~2.5) for optimum conversion, but below the critical ratio (~4.5) for spectral broadening and multimode operation. Under this condition, 5.1 W of single-mode signal and 3.5 W of single-mode idler were simultaneously generated for 14.5 W of pump at an overall extraction efficiency of nearly 60 percent, with a measured idler bandwidth of 30 kHz over 500 μs.

The advent of QPM nonlinear materials has had a profound impact on cw SROs, with the vast majority of devices developed to date based on PPLN as the nonlinear material. When pumped near ~1 μm by solid-state, amplified semiconductor, or fiber lasers, they can provide potential coverage from above ~1.3 μm up to the absorption edge of the material near ~5 μm. For wavelength generation below ~1.3 μm, the use of PPLN is generally precluded by photorefractive damage induced by visible pump or signal radiation. As such, the development of practical cw OPOs for visible and near-IR at wavelength below ~1.3 μm has remained difficult, particularly in high-power SRO configuration where strong visible pump and signal radiation are present. This has thus necessitated the use of additional frequency conversion schemes or deployment of alternative QPM materials such as PPKTP and, more recently, MgO-doped periodically poled stoichiometric $LiTaO_3$ (MgO:sPPLT). To extend the tunable range of cw SROs to the visible range, Strossner et al.[34] used an approach based on second harmonic generation (SHG) of the idler output from a cw SRO in an external enhancement cavity. By deploying a 10-W, single-frequency, cw pump laser at 532 nm in combination with multigrating PPKTP (L = 24 mm, Λ = 8.96 to 12.194 μm) and PPLN (L = 25 mm, Λ = 6.51 to 9.59 μm) crystals as the OPO gain medium, and PPLN (L = 43 mm, Λ = 6.51 to 20.93 μm) for SHG, a visible green-to-red tuning range of 550 to 770 nm in the frequency-doubled idler was demonstrated. Together with direct signal (656 to 1035 nm) and idler (1096 to 2830 nm) tuning, this resulted in a total system tuning range of 550 to 2830 nm, with a tuning gap of ~60 nm over 1035 to 1096 nm. The output power, limited by photorefractive damage to the PPLN crystal, and optical damage to the PPKTP crystal and coatings induced by input pump, was 60 mW (signal), 800 mW (idler), and 70 mW (visible frequency-doubled idler) for up to 3.3 W of pump. The output signal from the free-running SRO exhibited a short-term linewidth of 20 kHz over 50 μs, with a jitter of 300 kHz over 5 ms, and 5 MHz over 1 s. By frequency locking the SRO to a monolithic Nd:YAG laser, a jitter-free linewidth of 20 kHz was measured at a signal wavelength of 946 nm. In the absence of pump tuning, mode-hop-free tuning of SRO output was obtained by adjustment of the cavity length using piezo control and synchronous rotation of the etalon using a feedback loop, resulting in 38 GHz of fine tuning in the signal for PPKTP and 5 to 16 GHz for PPLN, limited by photorefractive effects. The

free-running SRO exhibited a mode hop over a free-spectral range (680 MHz) every 10 min, but locking the SRO cavity to the 532-nm pump ensured a long-term frequency drift of <50 MHz/h in the signal and idler, accompanied by a reduction in output power by ~10 percent.

More recently, the development of MgO:sPPLT has brought about new opportunities for the advancement of practical cw SROs for the visible and near-IR at wavelength below ~1.3 μm with the direct use of high-power solid-state laser sources in the green. By deploying a 10-W, single-frequency, cw, frequency-doubled Nd:YVO_4 pump laser at 532 nm, MgO:sPPLT (L = 30.14 mm, Λ = 7.97 μm) as the nonlinear crystal and temperature tuning, Samanta et al.[35] demonstrated a cw SRO with a tunable range of 848 to 1430 nm. Using a linear standing-wave cavity and double-pass pumping, the cw SRO had an oscillation threshold of 2.88 W, and could provide >1.51 W of single-pass idler power for 6 W of pump at an extraction efficiency of >25 percent and photon conversion efficiency of >56 percent. The maximum idler power and conversion efficiency in this SRO was limited by thermal lensing effects, attributed to the finite liner absorption of the green pump light in the MgO:sPPLT crystal. Despite this, the SRO could deliver >500 mW of single-pass power across the entire idler tuning range of 1104 to 1430 nm, and in a Gaussian profile, confirming the absence of photorefractive damage as is present in PPLN. With a standing-wave SRO cavity and in the absence of intracavity frequency selection, the output frequency in both signal and idler was characterized by mode hops. Soon after, by deploying a compact ring cavity with a 500-μm intracavity etalon, the authors demonstrated single-frequency operation of the cw SRO.[36] Using the same pump laser and MgO:sPPLT crystal in a single-pass pumping arrangement, the SRO had a pump power threshold of 2.84 W and could deliver 1.59 W of single-mode idler power over 1140 to 1417 nm for 7.8 W of pump at >20 percent extraction efficiency. The total SRO tuning range was 852 to 1417 nm, obtained for a variation in crystal temperature from 61 to 236°C. Under free-running conditions, the idler had an instantaneous linewidth of ~7 MHz and exhibited a peak-to-peak power stability of 16 percent over 5 hours. Measurements of idler power at different crystal temperatures revealed stronger thermal lensing at higher temperatures. In a separate experiment, operation of a similar cw SRO based on MgO:sPPLT and pumped by a Nd:YVO_4 laser at 532 nm was reported by Melkonian et al.,[37] providing tunable signal over 619 to 640 nm in the red. Using a ring cavity for the SRO containing a 30-mm multigrating crystal (Λ = 11.55 to 12.95 μm) and a 2-mm-thick intracavity silica etalon, the SRO could provide ~100 mW of nonresonant idler power. The resonant signal was extracted using a 1.7 percent output coupler, providing 100 mW of single-frequency red radiation for 10 W of input pump power. The cw SRO threshold varied from 3.6 W in the absence of the intracavity etalon up to 6.6 W with signal output coupling, and rising to 6.8 W depending on the exact signal wavelength. The maximum pump depletion was 15 percent, limited by thermal effects attributed to pump and signal absorption. The output signal frequency could be mode-hop-tuned over a total range of 27 GHz by rotation of the intracavity etalon, in steps of 255 MHz corresponding to free-spectral-range of the SRO cavity. With active stabilization of SRO cavity length, a frequency stability of 20 MHz over 3 min was obtained for the signal.

The development of practical, high-power, single-frequency cw SROs based on MgO:sPPLT pumped in the green and operating below 1 μm[35–37] has also provided new motivation for spectral extension to shorter wavelengths. By using internal SHG of the resonant near-IR signal in a cw SRO based on MgO:sPPLT, Samanta and Ebrahim-Zadeh[38] demonstrated the first cw SRO tunable in the blue. A schematic of the SRO configuration is shown in Fig. 10. The device was based on similar experimental design as in Ref. 36, except for the exclusion of the intracavity etalon and inclusion of a 5-mm BiB_3O_6 (BIBO) crystal at the secondary waist of the bow-tie SRO ring resonator to frequency double the circulating signal radiation in a single direction. By varying the temperature of the MgO:sPPLT crystal to tune the signal over 850 to 978 nm, and simultaneous rotation of the BIBO phase-matching angle, a wavelength range of 425 to 489 nm in the blue was accessed. The generated blue power varied from 45 to 448 mW across the tuning range, with the variation arising from the non-optimum reflectivity of the blue coupling mirror over the signal wavelength range. The output power behavior and pump depletion of the SRO with pump power is shown in Fig. 11. The frequency-doubled SRO had a threshold of 4 W (2.4 W without the BIBO crystal), and exhibited a pump depletion of up to ~73 percent under blue generation. In addition to the blue, the device could provide in excess of 100 mW of signal and as much as 2.6 W of idler output power. Without an intracavity etalon, the

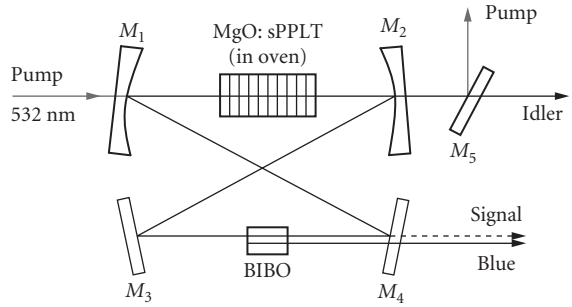

FIGURE 10 Schematic of the intracavity frequency-doubled MgO:sPPLT cw SRO for blue generation.[38]

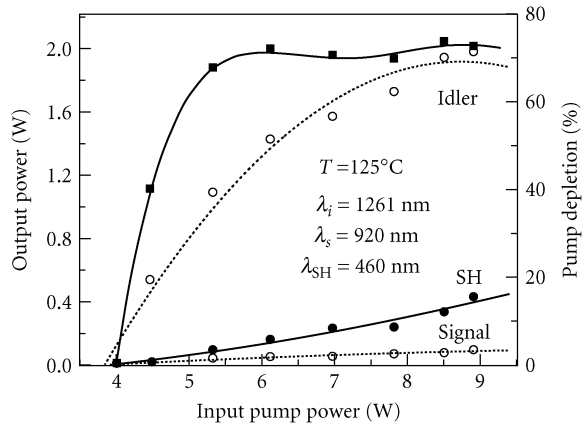

FIGURE 11 Single-frequency blue power, signal power, idler power, and pump depletion as functions of input pump power to the frequency-doubled cw SRO. Solid and dotted lines are guide for the eye.[38]

single-mode nature of the pump and resonant signal resulted in single-frequency blue generation and a measured instantaneous linewidth of ~8.5 MHz in the absence of active stabilization. The blue output beam also exhibited a gaussian spatial profile. In the meantime, operation of a intracavity frequency-doubled cw SRO based on MgO:sPPLT was also reported by My et al.,[39] providing tunable output in the orange-red. By resonating the idler wave in the 1170 to 1355 nm range in a ring resonator and employing a 10-mm intracavity β-BaB_2O_4 (BBO) crystal for doubling, tuning output over 585 to 678 nm was generated. With a 30-mm MgO:sPPLT crystal (Λ = 7.97 μm), up to 485 mW of visible radiation was internally generated for 7.6 W of pump, with 170 mW extracted as useful output. The device could also provide up to 3 W of nonresonant infrared signal power. The power threshold for the cw SRO was 4.5 W (4 W without the BBO crystal) and pump depletions of ~80 percent were measured for input powers >6 W. Without active stabilization, the visible SHG output was single mode with a frequency stability of 12 MHz over 12 min, and mode-hop-free operation could be maintained over several minutes.

In a departure from conventional cw OPOs based on bulk materials, the use of guided-wave nonlinear structures can also in principle offer an attractive approach to the realization of OPO sources in miniature integrated formats. The tight confinement of optical waves in a waveguide can

provide substantial enhancement in nonlinear gain per input pump power compared with the bulk materials, but a major drawback of the approach is the unacceptably high input and output coupling losses in the waveguide, hindering OPO operation. The problem is further exacerbated in the cw regime, and in the SRO configuration, which is characterized by the highest oscillation threshold. In an effort to overcome this difficulty, Langrock et al.[40] deployed the technique of fiber-feedback to achieve operation of a cw SRO based on a reverse-proton-exchanged (RPE) PPLN waveguide. In this approach, the SRO cavity was formed in a ring using a single-mode optical fiber pigtailed to both ends of the waveguide, providing feedback at the resonant signal wave. The pump was similarly coupled into the PPLN waveguide using a separate fiber and, together with the nonresonant idler, exited the waveguide in a single pass. The configuration resulted in minimum coupling losses of 0.7 dB (signal input) and 0.6 dB (signal output), and alignment-free operation. Using a 67-mm RPE PPLN waveguide containing a 49-mm grating (Λ = 16.1 μm), and a tunable external cavity diode laser at 779 nm as the pump, cw SRO threshold was reached at ~200 mW of coupled pump power. The waveguide cw SRO exhibited gain bandwidths in excess of 60 nm. Ultimately, however, practical realization of such waveguide cw SROs offering significant output will require further optimization of waveguide fabrication process to minimize propagation losses (α = 0.2 dB/cm) and loop losses (1.5 dB) in the present device, as well as further reductions in the waveguide-to-fiber coupling losses.

Multiple-Resonant Oscillators

Because the high pump power requirement for cw SROs can be prohibitive for many practical applications, extensive efforts have been directed to the development of cw OPOs in alternative resonance configurations, from the traditional DRO to the more recently devised PE-SRO and TRO, with the goal minimizing the pump power thresholds. These efforts have brought the operation of cw OPOs within the reach of more commonly available low- to moderate-power cw laser sources, albeit at the expense of added system complexity arising from the need for more elaborate cavity designs, more complex tuning protocols and the imperative requirement for active stabilization and control. In particular, the use of DRO and PE-SRO resonance schemes in combination with novel cavity designs have led to the practical generation of cw mid-IR radiation with the highest degree of frequency stability, and continuous mode-hop-free tuning capability over extended frequency spans at practical powers. These efforts have led to the realization of novel cw OPO systems in PE-SRO, DRO, and TRO configurations pumped by a variety of laser sources. These sources offer practical cw output powers in the mW to 100s mW range, high frequency stability, significant mode-hop-free tuning capability and extended wavelength coverage in the 1 to 5 μm spectral range.

Doubly Resonant Oscillators The use of DRO configurations in combination with PPLN has permitted substantial reductions in cw pump power threshold in cw OPOs, to levels compatible with the direct use single-mode semiconductor diode lasers, without the need for power amplification. The smooth wavelength tuning capability of the diode laser pump can then be similarly exploited to achieve continuous mode-hop-free tuning of the DRO output. In an example of such an approach, Henderson et al.[41] demonstrated a PPLN cw DRO pumped directly with a 150-mW, single-mode, single-stripe, DBR diode laser at 852 nm. Configured in a single, linear, standing-wave resonator and using a 19-mm-long multigrating crystal (Λ = 23.0 to 23.45 μm), the DRO exhibited a pump power threshold of ~17 mW, with thresholds as low as 5 mW under optimum alignment and minimum output coupling. Using three DRO mirror sets, a signal (idler) wavelength range of 1.1 to 1.4 μm (2.2 to 3.7 μm) was accessed by temperature tuning the PPLN crystal. The DRO generated a total signal and idler power of 18 mW at 1.3 and 2.3 μm, respectively, for 89 mW of input diode pump power, with 4 mW of output in the idler beam. Continuous mode-hop-free tuning of the signal (idler) at 1.3 μm (2.3 μm) could be obtained over 12 GHz (7 GHz) by smooth tuning the frequency diode laser using temperature variation and over 17 GHz (10 GHz) using current control in combination with active servo control of the DRO cavity length to follow the pump frequency scan. The continuous mode-hop-free tuning ranges were limited by the restrictions on DRO cavity length variation imposed by the piezoelectric transducer. With a pump linewidth of <3 MHz, the signal wave was measured to have

a linewidth of <7 MHz and a free-running frequency stability of ~20 MHz over 10 s without active stabilization. To demonstrate the utility of the diode-pumped cw DRO, continuous tuning of the idler was used in single-pass absorption spectroscopy of R6 line in CO gas at 2.3 μm.

In an effort to extend the wavelength coverage of cw OPOs to the visible spectrum, Petelski et al.[42] demonstrated a DRO tunable in the yellow, using a cascaded frequency scheme comprising three resonators including two external enhancement cavities, and a cw single-frequency monolithic ring Nd:YAG laser as the primary pump source. The pump light at 1.064 μm was frequency doubled in an external enhancement cavity using MgO:$LiNbO_3$ as the nonlinear crystal, to provide the input radiation for the cw DRO based on an identical crystal. With a threshold of 15 mW, the DRO delivered 95 mW of idler power for 450 mW of input at 532 nm, with the idler tunable over 1.130 to 1.190 μm by changing the temperature of the MgO:$LiNbO_3$ crystal. The generated idler output was then frequency doubled in an external enhancement cavity based on a 16-mm PPLN crystal (Λ = 8.0 to 8.6 μm) to provide tunable radiation across the 565 to 590 nm range. For 1.05 W of primary pump power at 1.064 μm, an output power of 3.8 mW was obtained at 580 nm, with active stabilization of the DRO and enhancement cavities providing single-mode output with a 3 percent intensity noise and stable operation over 10 hours. Fine tuning of the yellow output was obtained by smooth tuning of the Nd:YAG pump source, as well as mode-hop tuning of the DRO by scanning the cavity length. By tuning the pump frequency over 10 GHz, the yellow output at 580 nm was tuned continuously over 18 GHz, while mode-hop tuning could provide 160 GHz of step tuning across 20 mode pairs.

Pump-Enhanced Singly Resonant Oscillators In separate experiments, using a single-mode, single-stripe, grating-stabilized AlGaAs diode lasers at ~810 nm in both solitary and external-cavity configurations, Lindsay et al.[43] demonstrated a PPLN cw OPO in pump-enhanced configuration. Using a single, linear, standing-wave cavity for the OPO and a 50-mm, multigrating (Λ = 21.0 to 22.4 μm) crystal, a typical pump power threshold of 25 to 30 mW over a signal (idler) tuning range of 1.06 to 1.19 μm (2.58 to 3.44 μm) was demonstrated, with ~4 mW of single-mode idler power available for 62 mW of pump. Wavelength tuning could be achieved by the variation of pump wavelength, PPLN crystal temperature, or grating period. In the external cavity configuration, locking of the OPO cavity length to the pump laser frequency using the Pound-Drever technique enabled stabilized single-mode operation with a signal (idler) intensity fluctuation of ±3.5 percent (2.6 percent) at 0.5 mW (4 mW) power level over 1 hour. Over this period, pump frequency fluctuations of ±125 MHz resulted in ±100 MHz variation in signal frequency. However, mode-hop-free operation was maintained throughout the entire period. By continuous tuning of the external cavity diode laser over 510 MHz, a mode-hop-free tuning range of 377 MHz for the signal and 133 MHz for the idler was obtained, limited by the relative tuning rate of parametric gain curve and resonant signal modes with frequency tuning of the pump in the common-cavity PE-SRO, and so could be extended using a dual-cavity arrangement for the OPO.

By deploying a single-frequency cw Ti:sapphire pump laser, Turnbull et al.[44] demonstrated a cw PE-SRO based on a multigrating PPLN crystal (L = 19 mm, Λ = 21.0 to 22.4 μm) with an extended mid-IR idler coverage to 5.26 μm, well into the strong absorption region of the material beyond ~4.5 μm. The PE-SRO could provide idler tuning in two regions from 2.71 to 3.26 μm and from 4.07 to 5.26 μm, using a combination of temperature tuning and grating period variation. The oscillator exhibited a typical cw pump power threshold of 100 mW, increasing to more than 500 mW near 5 μm. For 750 mW of input pump power, the PE-SRO could typically provide a maximum one-way cw idler power of 16 mW. By employing a dual-cavity arrangement for the PE-SRO and a solid etalon in one arm of the resonant signal cavity, the authors were able to demonstrate mode-hop-free tuning of the idler over 10.8 GHz by smoothly tuning the pump laser over 12.3 GHz. In a further experiment, Stothard et al.[45] extended operation of the same PE-SRO to a single-cavity, traveling-wave ring geometry with the aim of extending the total fine-tuning performance of the oscillator and improving the idler output power. By using a low-finesse intracavity etalon to control the resonant signal frequency, the authors were able to achieve discontinuous mode-hop tuning of the idler frequency across the entire free spectral range of the etalon, corresponding to 83 GHz. The PE-SRO exhibited an oscillation threshold of 250 mW and could generate 35 mW of cw single-frequency mid-IR

idler radiation in the 2.8 to 3-μm spectral range for 600 mW of input Ti:sapphire pump power. In a separate experiment, Lindsay et al.[46] reported the operation of a cw PE-SRO based on PPRTA (L = 20 mm, Λ = 39.6 μm) as the nonlinear crystal. The PE-SRO was pumped by a diode-pumped cw single-frequency Nd:YVO_4 laser at 1.064 μm and was configured in a linear standing-wave resonator with the nonresonant idler double-passed through the cavity. With the 20-mm crystal length, the oscillator had an external pump power threshold of 250 mW and could deliver 87 mW of cw mid-IR idler output for 900 mW of input pump power. Coarse tuning of the idler over the wavelength range of 3.245 to 3.520 μm was achieved by temperature tuning the single-grating PPRTA crystal. Continuous mode-hop-free tuning of the PE-SRO over 0.7 GHz was also demonstrated by fine tuning the Nd:YVO_4 pump laser frequency.

In subsequent experiments, Muller et al.[47] investigated long-term frequency stability and linewidth properties of cw PE-SROs in common-cavity and dual-cavity configurations. Using multigrating PPLN crystals (L = 50 mm, Λ = 28.64 to 30.16 μm), a 2.5 W cw Nd:YAG pump laser (linewidth ~1 kHz/100 ms, frequency drift ~1 MHz/min) at 1064 nm, and linear standing-wave cavity arrangements for both configurations, they studied frequency stability and linewidth of the idler output tunable in the 3.1 to 3.9 μm spectral range. Schematics of the experimental setups for both cavity configurations are shown in Figs. 12 and 13. In the common-cavity PE-SRO (Fig. 12) with the pump and signal resonant in the same cavity, the OPO was locked to the pump laser using the Pound-Drever-Hall (PDH) technique, and the oscillator exhibited a threshold of 280 mW. In dual-cavity arrangement (Fig. 13), the pump and signal were resonated in separate linear cavities, with an intracavity 500-μm-thick Nd:YAG etalon inserted into the signal cavity for improved frequency control. The pump cavity was locked to the pump laser using the PDH method, while the signal cavity was locked to the point of maximum idler power using an intensity lock without an external reference. The use of dual-cavity configuration increased the threshold to 380 mW, but resulted in stable, mode-hop-free operation over 30 min. While an intrinsic advantage of the common-cavity PE-SRO is direct stabilization of the signal frequency to pump, it is more sensitive to mechanical perturbations, leading to mode hops. Moreover, reliable mode-hop-free operation and continuous frequency tuning by tuning the pump laser are more difficult due to the simultaneous resonance of two different wavelengths within a single cavity. On the other hand, the dual-cavity approach can overcome spontaneous mode hops and continuous tuning limitations of common-cavity PE-SROs, and can also offer several tuning methods combining etalon, signal cavity and pump frequency tuning. The

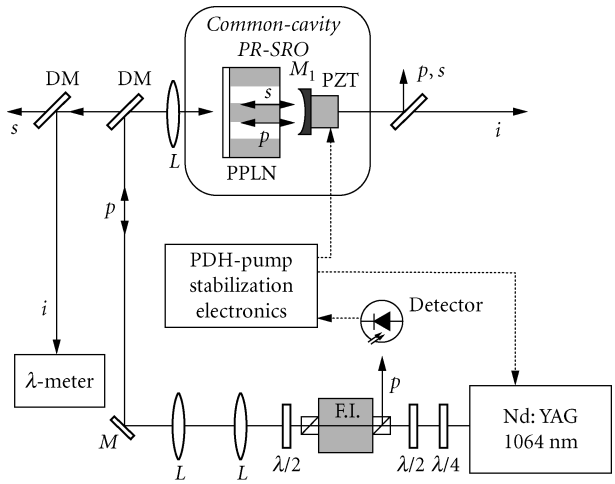

FIGURE 12 Common-cavity cw PE-SRO setup; M = mirror, DM = dichroic mirror, FI = Faraday isolator, L = lens, p = pump, s = signal, i = idler.[47]

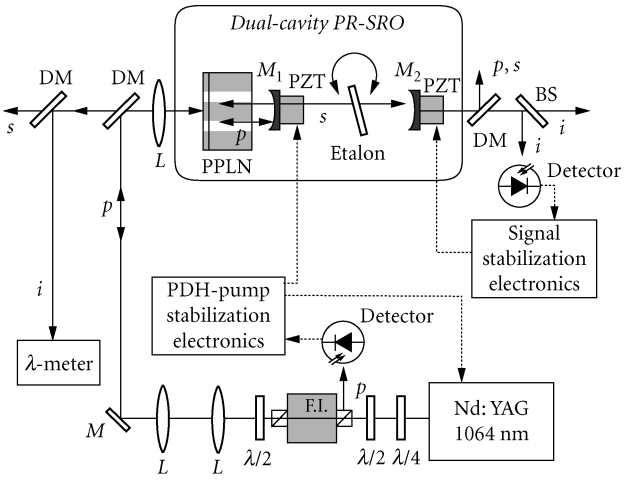

FIGURE 13 Dual-cavity cw PE-SRO setup; M = mirror, DM = dichroic mirror, FI = Faraday isolator, L = lens, p = pump, s = signal, i = idler.[47]

results of the investigations revealed long-term frequency stability better than ± 30 MHz over more than 30 min for both configurations (Figs. 14 and 15), limited by the resolution of the wavemeter. The short-term frequency jitter was 56 kHz over 1.8 s for the common-cavity PE-SRO and 13.5 MHz over 1.5 s for the dual-cavity PE-SRO. The short-term linewidths, measured using the cavity leak-out technique in external high-finesse cavities, were (9 ± 2) kHz for the common-cavity and (6 ± 1) kHz for the dual-cavity over 20 μs. The difference in frequency stability and linewidth of the two configurations is a result of the stabilization methods used. In the common-cavity PE-SRO, direct locking of the cavity to the pump laser provides a strong stabilization of the signal to pump frequency. In the

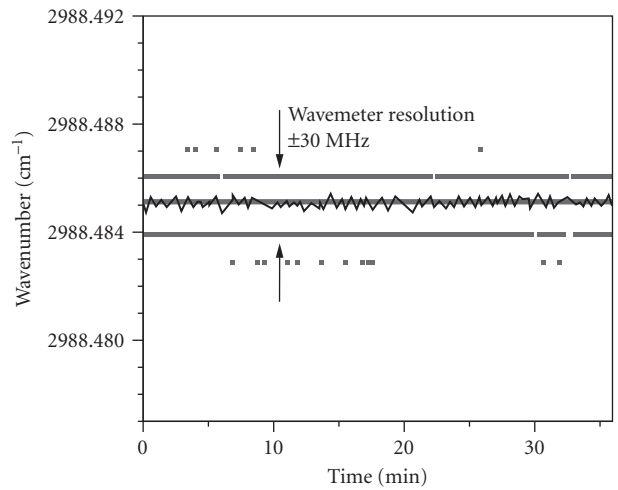

FIGURE 14 Long-term frequency stability (digital wavemeter read-out in 30 MHz steps and running average over 20 points) of the common-cavity cw PE-SRO.[47]

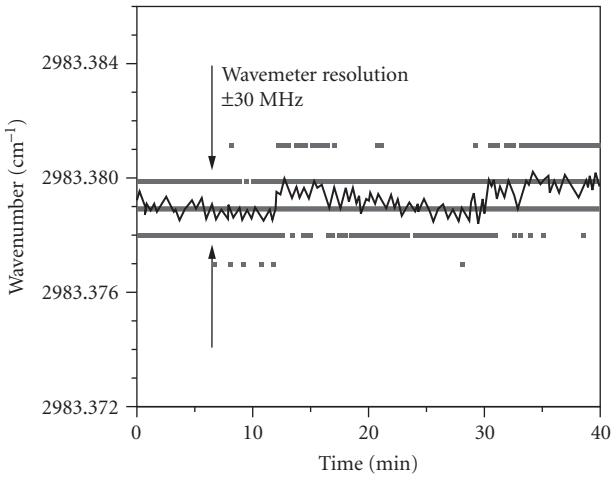

FIGURE 15 Long-term frequency stability (digital wavemeter read-out in 30 MHz steps and running average over 20 points) of the dual-cavity cw PE-SRO.[47]

dual-cavity PE-SRO, the signal cavity is locked to the maximum idler output power and so the idler frequency is coupled to the maximum of the phase-matching gain curve. Any shifts in the gain curve in time will also result in corresponding variations in the signal and idler frequencies. However, the reported results confirm that despite this limitation, the dual-cavity PE-SRO provides the required frequency stability and linewidths as well as continuous mode-hop-free tuning necessary for high-resolution spectroscopy.

Triply Resonant Oscillators Characterized by the lowest oscillation threshold, the TRO represents the least demanding configuration for cw OPOs with regard to pump power. However, practical operation of such oscillators requires active cavity length control to maintain simultaneous resonance of the pump, signal and idler within the OPO resonator. In an example of such a device, Gross et al.[48] reported a TRO based on a 58-mm PPLN crystal using only 14 mW of pump power from a grating-stabilized, single-frequency, extended-cavity diode laser at 805 nm. By deploying a linear two-mirror cavity, highly reflecting mirrors, optimum mode-matching and active stabilization, they achieved a threshold pump power as low as 600 μW at resonance, with a maximum total (signal and idler) output power of 47 μm generated for 13.5 mW of pump. With mirrors of higher transmission (4 percent) at the signal and idler, a total output power of 2.1 mW was generated for 13.8 mW of pump, but at the expense of an increase in pump power threshold to 4.5 mW. Using a segmented design for the PPLN crystal consisting of two 19-mm outer sections poled with multiple grating of identical periods (Λ = 20.2 to 20.8 μm) at 50 percent duty cycle and a single-domain section of length 20 mm at the centre, they demonstrated electro-optic tuning of the TRO output wavelengths at a fixed temperature, grating period, and pump wavelength. By applying an electric voltage of up to +1230 V across the single-domain section, wavelength tuning of the signal and idler over 1560 to 1660 nm could be obtained through modification of the phase-matching gain spectrum induced by the electro-optic effect. By applying a voltage modulation of amplitude 513 V at 0.11 Hz, signal (idler) tuning over 9.7 nm (10.8 nm) was demonstrated over 4.6 s, limited by the bandwidth of servo electronics.

Because of their phase coherent properties and the ability to generate exactly correlated frequencies, cw OPOs are also uniquely versatile sources for applications in optical frequency synthesis and metrology. Combined with compact solid-state semiconductor, or fiber pump lasers, they can offer practical tools for precision frequency generation, measurement, and control across extended regions spanning

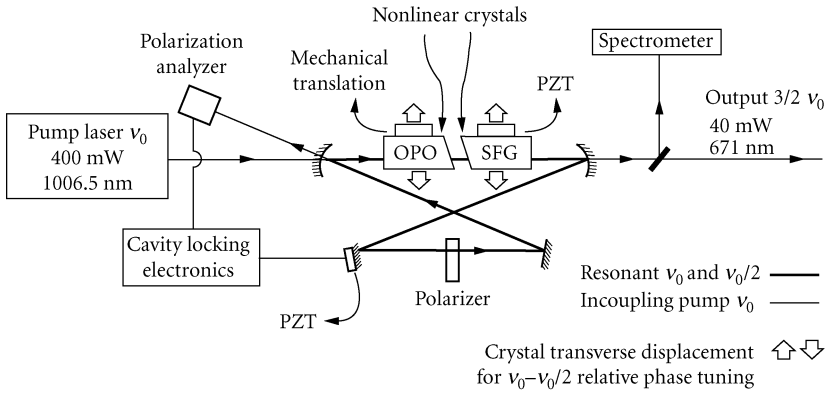

FIGURE 16 Schematic of the cw TRO for 3/2 frequency multiplier, converting a cw single-frequency radiation at 1006.5 nm into 671 nm. The wedged surfaces of the crystals are cut at an angle of 100 mrad with respect to the crystal axis. The input (output) facet of the OPO (SFG) crystal is at normal incidence. The two inclined surfaces facing each other are parallel. The transverse displacement of the nonlinear crystals provides an independent control over the cavity dispersion, ensuring simultaneous resonance of the two infrared fields.[49]

the optical spectrum. In a report, Ferrari[49] demonstrated a particular architecture for optical frequency synthesis based on a cw OPO in TRO configuration. By taking advantage of the lowest oscillation threshold offered by the TRO, the author developed a 3/2 pump frequency multiplier from the near-IR to visible using a 400-mW, single-mode semiconductor MOPA device at 1006.5 nm as the pump source (Fig. 16). The TRO, based on PPKTP as the nonlinear crystal (L = 20 mm, Λ = 38 μm), was operated at degeneracy to provide identical signal and idler frequencies at half the pump frequency. A second intracavity PPKTP crystal (L = 20 mm, Λ = 19.8 μm) was then used to sum the pump with the degenerate frequency, resulting in 3/2 frequency multiplication of the pump, corresponding to a wavelength of 671 nm in the red. To provide stable operation, the TRO cavity length was locked using the pump resonance, and independent control of the degenerate signal and idler oscillating modes was obtained by using wedged crystals. Fine tuning of the TRO cavity modes could be obtained while maintaining pump resonance by lateral translation of the wedged crystals to alter in the optical path lengths within the crystals, thus enabling single-frequency operation to be achieved at degeneracy. The TRO had a threshold of <50 mW and could provide 40 mW of single-mode output at degeneracy in a near-gaussian spatial mode with an RMS amplitude noise of 1.4 percent (50 kHz bandwidth) over 3 min at full power.

17.3 APPLICATIONS

The important advances in cw OPOs over the last decade have led to the realization of a new generation of practical coherent light sources in new spectral regions from the visible to the near- and mid-IR offering unprecedented optical powers, high frequency stability and narrow linewidth, excellent beam quality, and extended fine and coarse tuning. These capabilities have paved the way for the deployment of cw OPOs in new application areas, in particular spectroscopy. Most notably, cw OPOs based on PPLN have found important applications in sensitive detection and analysis of trace gases in mid-IR, where a variety of important molecular finger prints exist. A wide range of experiments, from simple single-pass absorption to high-resolution Doppler-free and cavity leak-out spectroscopy have been successfully performed by deploying cw OPOs based mainly on PPLN and operating in different resonance configurations of SRO, PE-SRO, or DRO. The higher cw output powers available to SROs and PE-SROs have also enabled detection of trace gases in the mid-IR with unprecedented sensitivity using photoacoustic spectroscopy.

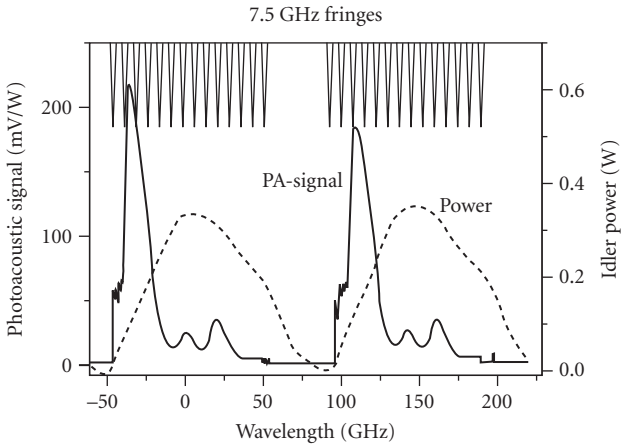

FIGURE 17 100-GHz-wide mode-hop scan of 10 ppm ethane in nitrogen was made around 2996.9 cm^{-1}. The solid line at the bottom shows the photoacoustic signal, the dashed line the idler power and the solid line at the top the fringes from a 7.5-GHz external Fabry-Perot etalon.[21]

By exploiting fine frequency tuning in a diode-pumped PPLN cw SRO, Klein et al.[28] performed single-pass absorption spectroscopy of rovibrational transitions in N_2O gas near 2.1 μm. The wide and continuous mode-hop-free tuning of the idler over 56 GHz enabled monitoring of three molecular lines separated by ~20 GHz within a single frequency scan.

Using a cw SRO based on PPLN, providing 700 mW of idler power and a total single-frequency fine tuning range of 24 GHz, Van Herpen et al.[20] recorded absorption line of ethane in nitrogen using the photoacoustic spectroscopy technique. In a later experiment,[21] by deploying a more powerful pump laser and a similar SRO configuration, photoacoustic spectroscopy of ethane in nitrogen was demonstrated with a detection sensitivity of 10 parts per trillion (ppt) (Figs. 17 and 18). The

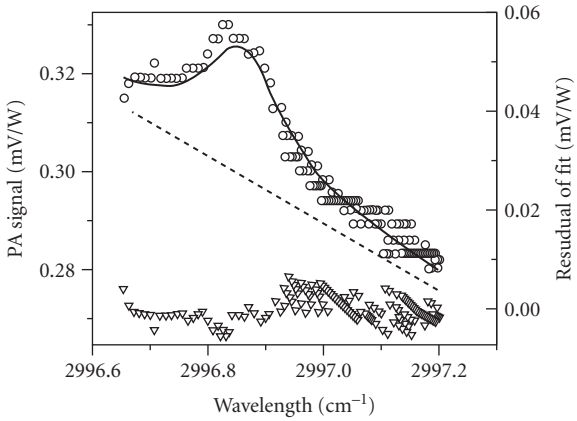

FIGURE 18 Pump-scan around 2996.^{9} cm^{-1} of 0.4-ppb ethane in nitrogen at atmospheric pressure. A lorentzian fit with linearly decreasing background has been plotted through the data (dashed line). The linearly decreasing background is also shown separately with a dotted line. The bottom of the picture shows the residual if the fit is subtracted from the data.[21]

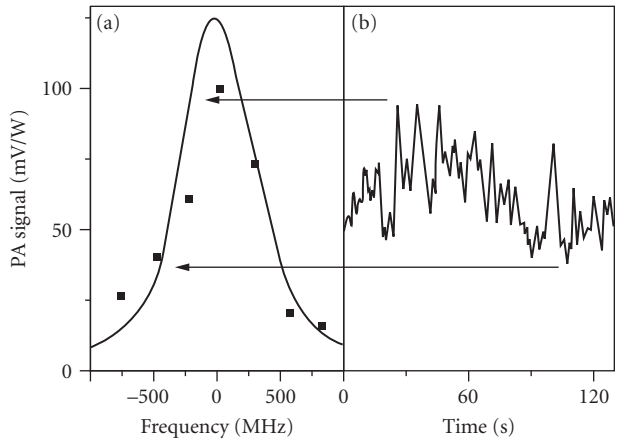

FIGURE 19 The high resolution performance and the wavelength stability of the SRO are demonstrated by recording the photo acoustic signal from the half maximum of a 77 mbar pressure broadened absorption line of 20 ppm of ethane in nitrogen at 2996.9 cm^{-1}. When not tuning the pump frequency, the photoacoustic signal shows random oscillations at a rather high frequency (90 MHz/s), combined with an oscillation at a lower frequency (250 MHz in 200 s).[23]

extension of operation of the SRO to the 3.7 to 4.7-μm spectral range enabled photoacoustic detection of the CO_2 absorption line in nitrogen near 4.235 μm using 24-GHz continuous scan of the idler frequency.[22] By using a high-power cw SRO based on PPLN operating in the 2.6 to 4.7 μm in the mid-IR, photoacoustic spectroscopy of a mixture of 20-ppm ethane in nitrogen was performed near 3.33 μm.[23] The SRO was pumped by a 20-W, cw single-frequency Yb:YAG laser (tunable over 1.024 to 1.034 μm) and could deliver 3 W of idler power at 2.954 μm (Fig. 3). By step-tuning the pump frequency using a combination of intracavity etalon and a Lyot filter, mode-hop-tuning of the idler over 190 GHz could be achieved, enabling coverage of several absorption lines of ethane. With 2.15 W of idler power available at 3.33 μm, a photoacoustic detection sensitivity of 0.005 ppb was deduced. By monitoring the photoacoustic signal corresponding to the strongest absorption peak in the same 20-ppm mixture of ethane in nitrogen at low pressure (77 mbar) as a function of time (Fig. 19), a slow idler frequency drift of 250 MHz over 200 s was measured, which was attributed to the fluctuations in the PPLN crystal temperature and lack of thermal isolation of the SRO from the environment. The idler frequency also exhibited fast frequency fluctuations of 90 MHz/s, attributed to the nonoptimized coatings of the PPLN crystal and cavity mirrors, which resulted in unwanted etalon and resonance effects in the SRO cavity. In a later report, Ngai et al.[24] performed photoacoustic and cavity leak-out spectroscopy of several trace gases including CO_2 and multicomponent gas mixtures of methane, ethane, and water in human breath using an automatically tunable cw SRO based on a multigrating MgO:PPLN crystal (Figs. 4 and 5). By deploying a ring SRO cavity with an uncoated intracavity YAG etalon and using a combination of pump tuning and etalon rotation, step-tuning of the idler over 207 GHz could be achieved. Adjustment of the crystal temperature could further be used to repeat this process, to provide wavelength scans of up to 450 cm^{-1} with a single grating period at high resolution ($<5 \times 10^{-4}$ cm^{-1}). By translating the crystal to other grating periods, an extended idler wavelength range of 2.75 to 3.83 μm could be accessed. Using the wide wavelength scanning capability, extended wavelength coverage, and automatic tuning capability of this source, photoacoustic spectroscopy of strong CO_2 combination bands in laboratory air (460 ppmv) extending over 14 nm (from 2788 to 2802 nm) was recorded by a combination of pump tuning, etalon rotation and crystal temperature tuning with a spectral resolution of 0.01 nm and a recording time of 1 hour. The recorded spectra were corrected for the water-vapor contribution to reveal the true

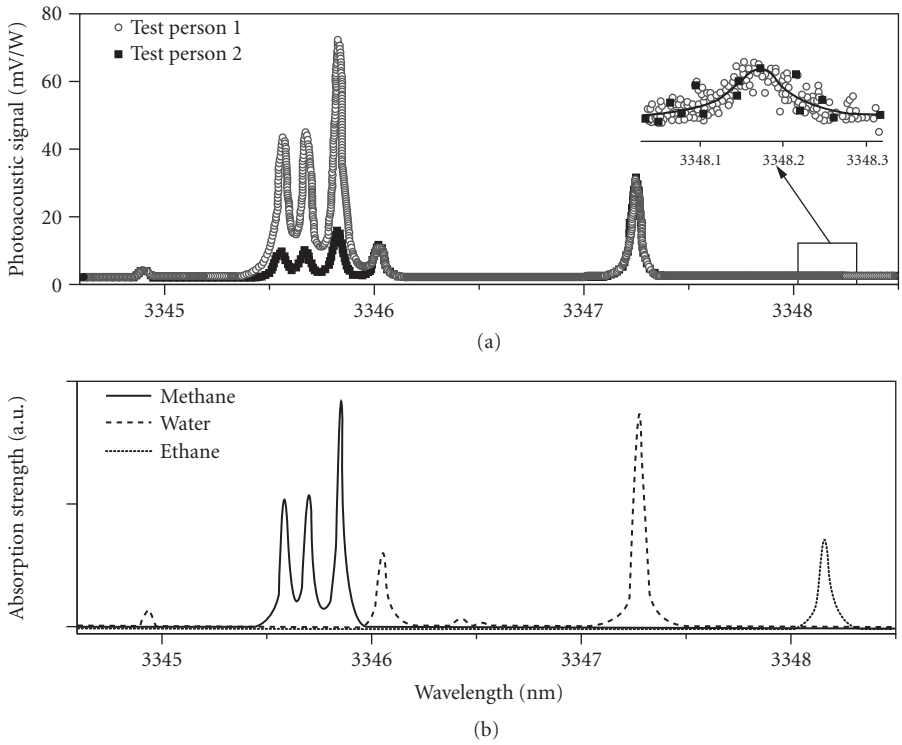

FIGURE 20 (*a*) Photoacoustic spectra measured from the breath of two different test persons. The recorded spectra reveal a higher methane concentration in the breath of person 1, indicating the presence of methanogenic flora. (*b*) Calculated absorption spectra based on the HITRAN database for methane, ethane, and water.[24]

CO_2 spectra, with the results in excellent agreement with calculations. Similarly, using the same automatic tuning protocol, photoacoustic spectroscopy of methane, ethane, and water vapor in human breath were simultaneously recorded by scanning the idler wavelength in the 3344 to 3349 spectral range (Fig. 20). Concentrations of 21 ppmv and 13 ppbv were calculated for methane and ethane, respectively, in the first sample, and 4.5 ppmv and 13 ppbv in the second sample. Using the same cw SRO, cavity leak-out spectroscopy was performed for gas mixtures containing methane (at 3.221 μm) and ethane (at 3.337 μm) in N_2 at 100 mbar pressure. In the case of methane, the absorption peak was scanned over 200 s with a spectral resolution of 0.001 cm^{-1}, resulting in a background methane concentration of 31 ppbv in N_2, a noise-equivalent detection limit of 0.16 ppbv, and a minimum detectable absorption coefficient of 2.0×10^{-9} cm^{-1}. For ethane, the idler was scanned over 60 s with a lower resolution of 0.01 cm^{-1}, resulting in concentrations from 5 to 100 ppbv, a noise-equivalent detection limit of 0.07 ppbv, and a minimum detectable absorption coefficient of 1.4×10^{-9} cm^{-1}. The cw SRO was also used to record the spectrum of $^{12}CH_4$ and $^{13}CH_4$ isotopes of methane in laboratory air with cavity leak-out spectroscopy. Scanning the idler wavelength from 3210 to 3211.5 nm revealed the absorption features corresponding to the two isotopes as well as water vapor, with the measured data in good agreement with calculated spectra.

The rapid and continuous mode-hop-free idler tuning over 110 GHz in a PPLN cw SRO pumped by a fiber-amplified DBR diode laser[29] has been used to perform real-time single-pass absorption spectroscopy of methane near 3.39 μm with a refresh period of 29 ms and a corresponding refresh rate of 34 Hz, demonstrating the suitability of the system for rapid spectroscopic measurements (Fig. 21). In a subsequent experiment,[50] by taking advantage of frequency modulation capabilities

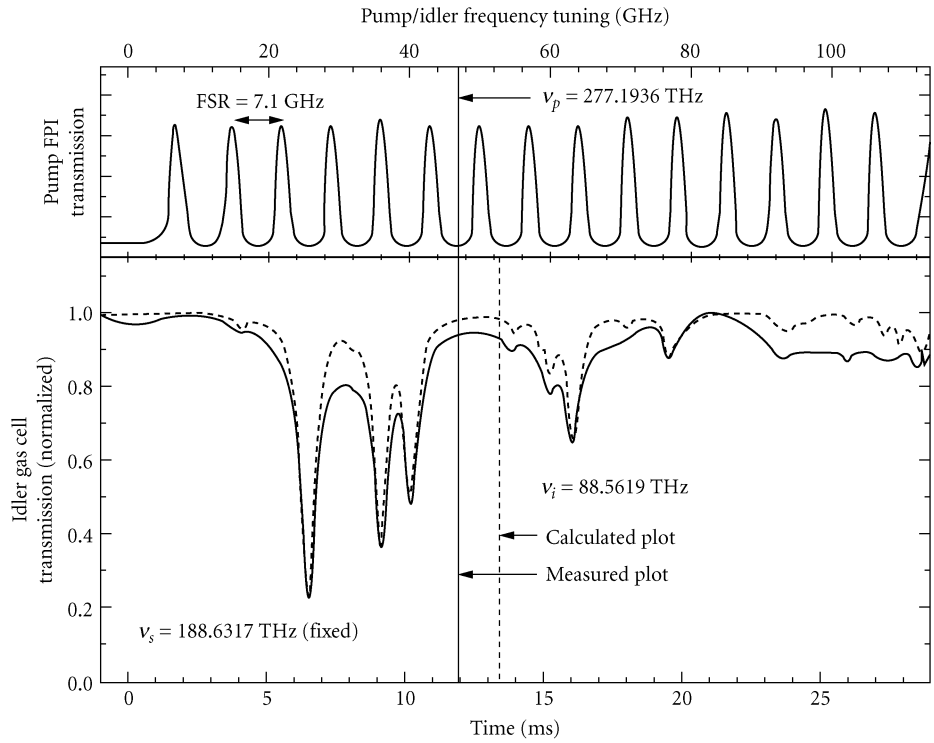

FIGURE 21 Rapid mode-hop-free tuning of a cw SRO pumped by a fiber-amplified DBR diode laser, and application absorption spectroscopy of CH_4.[29]

of the idler output from a similar fiber-amplified DBR diode-pumped cw SRO, sensitive detection of multicomponent trace gas mixtures was performed using quartz-enhanced photoacoustic spectroscopy (QEPAS). The SRO, based on a multigrating MgO:PPLN crystal (L = 50 mm, Λ = 28.5 to 31.5 μm), was similarly configured in a ring cavity with a 400-μm-thick uncoated intracavity YAG etalon to provide enhanced frequency selection and stability (Fig. 22). The pump laser delivered 7.9 W of single-frequency power at 1082 nm with a linewidth of ~100 MHz. The idler wavelength was tuned coarsely over 3 to 4 μm by a combination of grating and temperature tuning, in discrete steps of 1 to 4 cm^{-1} due to the combination of SRO cavity modes, etalon mode selection and phase-matching bandwidth of the crystal. Pump tuning was then used to provide fine wavelength control and mode-hop-free tuning of the idler over 5.2 cm^{-1}, which could be shifted within a total range of 16.5 cm^{-1} by current control of the DBR diode laser. By monitoring the idler wavelength with a wavemeter, and using a computer-controlled feedback loop to adjust the phase and current to the DBR, locking of idler frequency at 2990.076 cm^{-1} could be achieved with a stability of 1.7×10^{-3} cm^{-1} over 30 min. With the programmed tuning, idler wavenumbers from 2987 to 2994 cm^{-1} could be accessed in 1-cm^{-1} steps within the pump tuning range, with any desired wavelength reached within ~20 s of tuning the pump. Using this source, QEPAS spectral data of 2-ppmv ethane in nitrogen were successfully recorded at 2990.1 cm^{-1}, as well as isolated 1.2 percent water vapor at 2994.4 cm^{-1} (Fig. 23). By locking the pump laser frequency to the maximum ethane absorption peak at 2990.08 cm^{-1} and measuring concentrations from 20 ppmv down to 100 ppbv, a QEPAS detection limit of 25 ppbv was deduced. By keeping the idler wavelength fixed at the same absorption peak with a 2 ppmv methane concentration, a linear dependence of QEPAS signal on input power was verified, confirming the advantage of higher powers for improved detection sensitivity. To further demonstrate the

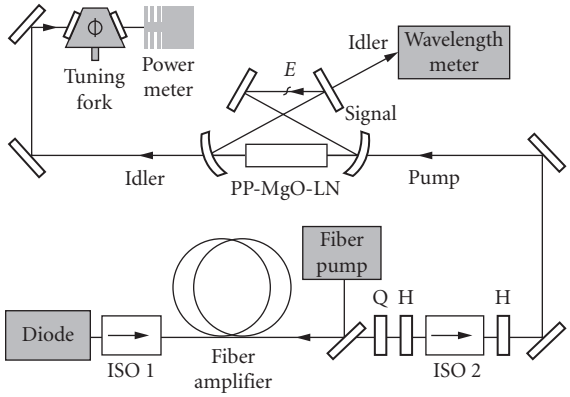

FIGURE 22 Schematic of the cw SRO experimental setup for quartz-enhanced photoacoustic spectroscopy.[50]

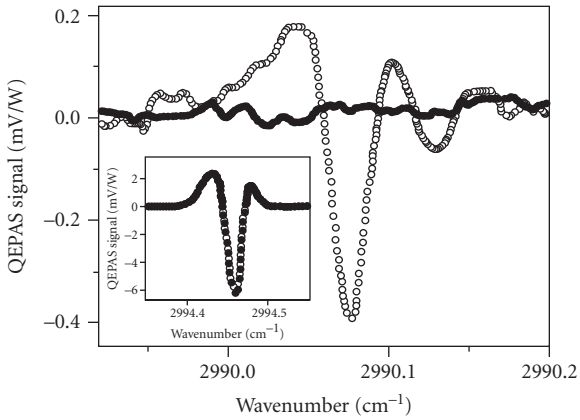

FIGURE 23 Example of a QEPAS scan over a 2 ppmv ethane peak at 2990.08 cm^{-1} (*open circles*) in 200 mbar nitrogen gas. QEPAS signal detected from pure nitrogen in the same spectral range is also shown, revealing a flat background signal (*filled circles*). Another example of a QEPAS scan is given in the *inset* for 1.2 percent water at 2994.4 cm^{-1}.[50]

unique advantages offered by the wide tuning coverage of the cw SRO, QEPAS data corresponding to a multiple gas mixture containing 2.2 ppmv ethane, 1.1 percent water, and 1.5 ppmv methane were successfully recorded by pump-tuning the idler from 2979.4 to 2994.6 cm^{-1}, with the obtained spectra in good agreement with calculations. From the obtained data, it was also possible to deduce an improved QEPAS detection limit of 13 ppbv for the stronger methane absorption line at 2983.3 cm^{-1} and 6.8 ppmv for water at 2994.4 cm^{-1}.

By deploying an all-fiber-pumped PPLN cw SRO,[27] single-pass absorption spectroscopy of several gases over the wavelength range of 2700 to 3200 nm was performed by continuous scanning of the idler frequency with a linewidth of ~1 MHz. Using piezoelectric tuning of the fiber pump laser allowed mode-hop-free tuning of the idler frequency up to 60 GHz, enabling high-resolution spectroscopy of various absorption features in water vapor (2709 nm), carbon dioxide (2810 nm), nitrous oxide (2879 nm), ammonia (2897 nm), and methane (3167 nm).

In a separate experiment, using a PPLN cw DRO pumped directly by a 150-mW DBR diode laser and delivering 4 mW of idler output with a mode-hop-free tuning range of 10 GHz, simple single-pass absorption spectroscopy of CO molecule at 2.3 μm was demonstrated.[41] Spectroscopic applications of cw OPOs in the visible spectral range has also been performed by external frequency doubling of the idler output from a cw DRO in an external enhancement cavity to generate yellow radiation in the 565 to 590 nm region.[42] The DRO was pumped by a cw, monolithic ring Nd:YAG laser at 1064 nm and by tuning the pump frequency over 10 GHz, the yellow output at 580 nm could be tuned smoothly over 18 GHz, while mode-hop tuning could provide 160 GHz of step-tuning across 20 mode pairs. This tuning capability enabled spectroscopy of the $^5D_0 \rightarrow {}^7F_0$ transition in $Eu3^+:Y_2SiO_5$ at 4 K, which is of interest because it exhibits the lowest known homogeneous linewidth for an optical transition in a solid. The step-tuning capability enabled the full spectrum of the transition containing two absorption peaks at 580.070 and 580.224 nm to be scanned, while the fine mode-hop-free tuning enabled continuous scan of each inhomogeneously broadened absorption peak, resulting in linewidths of $\Delta\nu = 3$ GHz and $\Delta\nu = 2.5$ GHz, respectively. Persistent spectral hole-burning was also observed by continuous tuning of the pump, and linewidths <1 MHz were recorded after 40 min of burning. By monitoring the hole spectrum every few hours, it was possible to follow the hole decay as long as 15 hours, demonstrating the repeatability of frequency tuning and stability of the cw DRO over many hours.

By deploying a cw PE-SRO based on a 19-mm-long PPLN crystal, Kovalchuk et al.[51] performed high-resolution Doppler-free spectroscopy of rovibrational transition of methane molecule at 3.39 μm. The PE-SRO, configured in semi-monolithic cavity design and containing an intracavity etalon, was pumped by a cw single-mode Nd:YAG ring laser with a linewidth of ~5 kHz. It could provide single-frequency idler output with a linewidth of ~100 kHz and a mode-hop-free tuning range of 1 GHz, obtained by smooth tuning of the pump laser. The PE-SRO had a minimum oscillation threshold of 305 mW and generated a total two-way idler power of 58 mW at 3.39 μm for 808 mW of input pump power. With this set-up, Doppler-free resonances with a resolution of ~500 kHz were recorded in methane, limited by the frequency jitter of the PE-SRO idler output and pressure broadening. Subsequently, Muller et al.[52] reported a transportable, all-solid-state photoacoustic spectrometer based on a cw PE-SRO using an alternative dual-cavity semi-monolithic cavity design. The PE-SRO used a 19-mm-long multigrating PPLN crystal and was pumped by a 2.5-W cw single-frequency Nd:YAG laser at 1.064 μm. The oscillator was characterized by a pump power threshold of 380 mW and could generate a total two-way idler power of 200 mW. Using active signal cavity length stabilization, an idler frequency stability better than ±30 MHz was obtained. Coarse tuning of the idler wavelength over 3.1 to 3.9 μm was performed by a combination of temperature and grating period variation, while the use of an etalon inside the signal cavity enabled continuous mode-hop-free tuning of the idler over 1.5 GHz by tuning the pump laser. Mode-hop tuning of the idler frequency in steps of 450 MHz could also be achieved over 52 GHz by rotation of the intracavity etalon. Using this mode-hop tuning method and with 70 mW of available idler power, photoacoustic spectroscopy of ethane was performed with a detection sensitivity of 110 ppt. By deploying the same dual-cavity cw PE-SRO in combination with cavity leak-out spectroscopy, substantial improvement in detection sensitivity of ethane down to 0.5 ppt was demonstrated near 3 μm,[53] and by exploiting the frequency tuning capability of the PE-SRO, simultaneous monitoring of ethane, methane, and water vapor in human breath could be performed, without significant interference from other gases.

In a further application, Stothard et al.[54] demonstrated the use of a cw PE-SRO for hyperspectral imaging of gases in the mid-IR. Based on a 20-mm-long, single-grating crystal of PPRTA and pumped by a 1-W diode-pumped $Nd:YVO_4$ laser, the PE-SRO could provide ~50 mW of idler output power and coverage in the 3.18 to 3.50-μm spectral range by temperature tuning the crystal. The use of a three-mirror standing-wave PE-SRO cavity and an intracavity etalon at the signal wavelength-enabled mode-hop tuning of the idler frequency over ~30 GHz, in steps of 1.4 to 2 GHz, by rotation of the etalon. This frequency resolution was sufficient compared to the typical linewidth of ~5 GHz for pressure-broadened transitions in gases under atmospheric pressure, thus enabling the deployment of the cw PE-SRO for imaging of methane gas in the atmosphere. By tuning the cw PE-SRO idler frequency to the strong methane absorption lines near 3.27 and 3.35 μm, gas concentrations of

the order of 30 ppm-m could be detected and significant target areas (~4 m^2 at 3 m) could be effectively imaged with the subsecond acquisition times.

As well as versatile spectroscopic tools, cw OPOs offer unique sources of correlated twin beams and nonclassical states of light for applications in quantum optics and quantum information processing. When pumped by cw all-solid-state lasers, they can provide compact twin-beam optical sources for quantum cryptography and sub-shot-noise measurement. In one configuration of such a device, a cw TRO based on a 10-mm KTP crystal and using a linear semi-monolithic resonator to separate the pump and parametric wave cavities, was reported by Hayasaka et al.[55] The TRO was pumped at 540 nm by the second harmonic of an extended-cavity single-stripe cw diode laser and was operated close to degeneracy. The use of this pump wavelength permitted type II NCPM in KTP, resulting in a TRO pump power threshold as low as 2.5 mW near degeneracy and providing 5.1 mW of cw output power for 16 mW of pump power. By recording the noise spectrum of the twin-beam intensities, 4.3 dB of intensity-difference squeezing was observed at ~3 MHz. In a subsequent experiment, Su et al.[56] demonstrated quantum entanglement between the signal and idler twin beams in a nondegenerate cw DRO above threshold. The DRO, based on a 10-mm PPKTP crystal cut for type II nondegenerate phase matching, was configured in a linear semi-monolithic cavity and was pumped by the stabilized cw single-mode output of a frequency-doubled Nd:YAP laser at 540 nm. Using a pair of unbalanced Mach-Zender interferometers with unequal arm lengths, the amplitude and phase noise of the signal and idler beams above threshold were recorded at 20 MHz, enabling quantum correlations to be deduced from the noise levels of the intensity difference and phase sum of the photocurrents measured by the unbalanced interferometers. Using this method, the authors were able to deduce correlations of amplitude and phase quadratures of signal and idler below the shot-noise-limit, amounting to ~2.58 and ~1.05 dB, respectively, and from the sum of the amplitude and phase correlation variances, demonstrate quantum entanglement of the twin beams below the shot-noise-limit. For 230 mW of input pump power, nearly twice the 120-mW DRO threshold, the output power in the correlated twin beams was 22 mW. The nondegenerate signal and idler twin beams were at wavelengths of 1079.130 and 1080.215 nm, respectively, separated by 1.085 nm. In another experiment, Tanimura et al.[57] deployed a cw DRO below threshold to generate squeezed vacuum on resonance with the rubidium *D* line at 795 nm. The DRO, based on a 10-mm crystal of PPKTP, was configured in a ring cavity and pumped at 397.5 nm by the second harmonic of a cw single-frequency Ti:sapphire laser to provide near-degenerate signal and idler frequencies at 795 nm (Fig. 24). Operating the cw DRO below threshold and using homodyne detection, the authors were able to measure strongly squeezed vacuum at the OPO output. With the DRO operated at 61 mW of input pump power, below a calculated threshold of 150 mW, a squeezing level of –2.75 dB below the shot-noise-limit and anti-squeezing level of +7.00 dB above the shot-noise-limit was observed (Fig. 25). Such a system could find useful applications for ultraprecise measurements of atomic spins as well as quantum information processing by mapping squeezed vacuum onto an atomic ensemble.

Because of their phase coherent properties and the ability to lock correlated frequencies to stable optical references, cw OPOs also represent highly promising light sources for applications in optical frequency synthesis and metrology. In an example of such application, a novel approach based on the combination of a cw OPO with a femtosecond Ti:sapphire frequency comb was used to provide a phase-coherent bridge from the visible to mid-IR spectral regions.[58] The cw PE-SRO, based on a 19-mm PPLN crystal and deploying a similar configuration to that in Ref. 51 was pumped by a cw single-frequency Nd:YAG laser. The oscillator provided idler emission in the 2.4 to 3.7-μm spectral range, with 50 mW of idler power and an instantaneous linewidth of ~10 kHz at 3.39 μm. The technique takes advantage of the fact that in a PPLN cw PE-SRO, in addition to the phase-matched signal and idler, there are also non-phase-matched frequencies generated by mixing of the resonant pump and signal waves. This process provides a range of visible frequencies within the emission bandwidth of a femtosecond Ti:sapphire laser, which can be used for frequency comparison with the nearest comb lines. By forming suitable differences of the heterodyne beat frequencies between the visible frequency components from the cw OPO and adjacent comb lines in the femtosecond laser, mutual phase locking of OPO optical frequencies, Ti:sapphire repetition frequency and carrier-envelope offset frequency could be obtained. Using this method, the authors performed direct frequency comparison between an iodine-stabilized Nd:YAG laser at 1.064 μm and a mid-IR methane

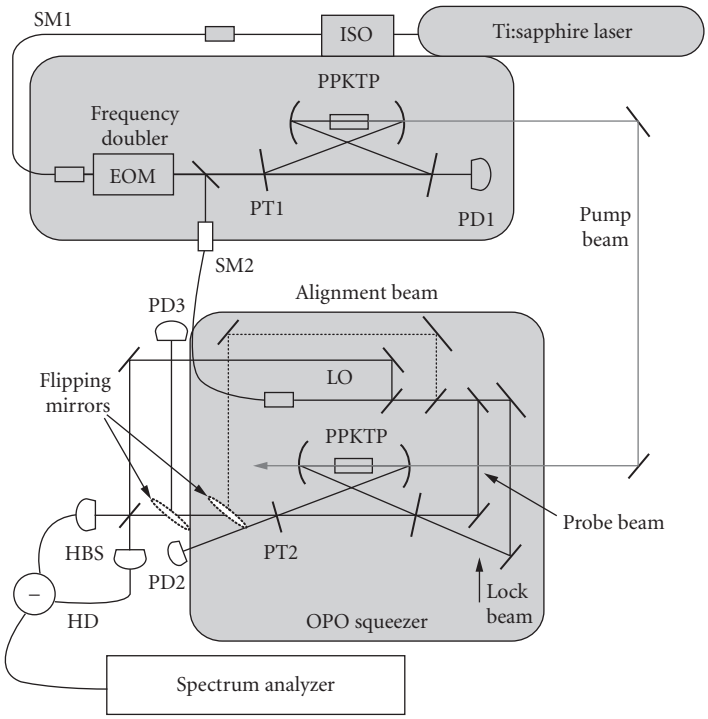

FIGURE 24 Experimental setup for PPKTP cw DRO for the generation of squeezed vacuum. ISO, optical isolator; EOM, electro-optic modulator; OPO, subthreshold degenerate optical parametric oscillator; HBS, half-beam splitter; PT, partial transmittance mirror; HD, balanced homodyne detector; PD, photodiode; SM, single-mode fiber.[57]

optical frequency standard at 3.39 μm. Subsequent demonstrations, taking advantage of the unique coherence properties of cw OPOs for frequency synthesis, include the development of a precise 3/2 frequency multiplier from a near-IR pump to the visible using a cw TRO.[49]

17.4 SUMMARY

This chapter has provided an overview of the latest advances in cw OPOs and their applications over the past decade. The advent of QPM nonlinear materials has had an unprecedented impact on cw OPO technology which, combined with major advances in solid-state laser technology and innovative design architectures, has led to the realization of a new generation of truly practical cw OPOs with performance capabilities surpassing conventional lasers. The mature technology and ready availability of PPLN has enabled the development of near- and mid-IR cw OPOs for the 1 to 5 μm spectral range in various resonance configurations, from TROs offering minimal oscillation threshold and lowest output power to cw SROs with highest threshold and watt-level output power, previously unattainable with birefringent nonlinear materials, and using a variety of pump sources from miniature semiconductor diode lasers to high-power solid-state and fiber lasers. The application of novel cavity designs and resonance schemes including pump enhancement, dual cavities and

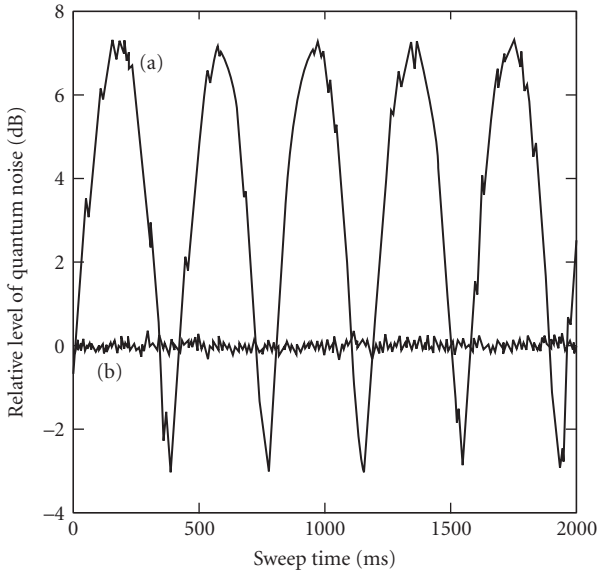

FIGURE 25 Measured quantum noise levels in cw DRO base on PPKTP. (*a*) Local oscillator beam phase was scanned. (*b*) Shot-noise level. Noise levels are displayed as the relative power compared to the shotnoise level (0 dB). The settings of the spectrum analyzer were zero-span mode at 1 MHz, resolution bandwidth = 100 kHz, and video bandwidth = 30 Hz.[57]

intracavity pumping, together with innovative tuning and stabilization techniques have enabled the generation of coherent output with excellent power and frequency stability and short-term linewidths down to a few kHz, long-term stability of a few MHz, and smooth mode-hop-free tuning of more than 100 GHz from cw OPOs. With the continuing advances in QPM material technology, reliable fabrication of MgO-doped PPLN has led to significant reductions in photorefractive damage, enabling its use at lower temperatures and higher powers with reduced output beam degradation. By deploying high-power fiber pump lasers in combination with MgO:PPLN, output powers in excess of 10 W have now been realized in cw SROs and power scaling to several tens of watts appears a clear possibility.

While photorefractive damage has placed limitations on the use of (MgO:)PPLN under visible pumping and confined operation of cw OPOs to near- and mid-IR above ~1 μm, advances in QPM material technology have enabled reliable fabrication of alternative QPM crystals with short grating periods, long interaction lengths, and immunity to photorefraction. This has paved the way for spectral extension of cw OPOs to the wavelengths below 1 μm by exploiting QPM materials including MgO:sPPLT and PPKTP and using direct pumping in the visible followed by additional frequency upconversion steps internal or external to the OPO cavity. By exploiting such techniques, spectral regions in orange and red have been successfully accessed and wavelengths down to 425 nm in the blue have been generated at several hundred milliwatts of output power in single-frequency spectrum and high beam quality. These developments have opened up new opportunities for the realization of practical solid-state sources with wide tunability across the visible and into the UV, where there is a severe shortage of conventional laser sources or other solid-state technologies.

The rapid advances in cw OPOs over the past decade have paved the way for the routine deployment of practical devices in a wide range of applications, from spectroscopy and imaging to frequency metrology and quantum optics. The unique capabilities of cw OPOs with regard to spectral versatility, output power, frequency and power stability, and compact solid-state design

open up new avenues for the ultimate development of these devices in real applications including portable gas detectors, mobile breath analyzers, handheld imaging systems or transportable optical frequency meters. At the same time, significant challenges and opportunities remain for further advancement of cw OPOs. In particular, wavelength extension of these devices into the mid-IR wavelength regions beyond 5 μm remains difficult because of the absorption of oxide-based QPM nonlinear materials, the key building blocks for the successful development of cw OPOs. The 5 to 12-μm spectral range is a particularly important and interesting region because of the presence of several atmospheric windows as well as many molecular absorption finger prints, including volatile substances in exhaled breath. The development of cw OPOs for this wavelength range will thus be of significant interest for spectroscopy, gas sensing, biomedicine, and atmospheric transmission. Progress toward the development of cw OPOs in this spectral range will require the deployment of alternative mid-IR birefringent nonlinear materials such as $ZnGeP_2$, or the more recently developed nonlinear crystals such as $CdSiP_2$ and orientation-patterned GaAs, together with suitable near- to mid-IR laser pump sources and cascaded two-step pumping schemes. On the other hand, advancement of cw OPOs toward shorter UV wavelengths below the current 425-nm limit will be feasible with the use of recently demonstrated frequency upconversion techniques internal to cw SROs by exploiting existing birefringent crystals such as BBO, BIBO, and LBO. With the rapid advances in cw fiber laser technology and the potential for wavelength extension toward the extremes of the optical spectrum, the realization of compact, high-power and practical coherent solid-state light sources across the entire 300 to 12000 nm range based on cw OPOs appears a clear possibility in not too distant a future.

17.5 REFERENCES

1. M. Ebrahim-Zadeh and M. H. Dunn, "Optical Parametric Oscillators," in *OSA Handbook of Optics*, Vol. 4, (McGraw-Hill, New York, 2000) pp. 22.1–22.72.
2. J. A. Giordmaine and R. C. Miller, "Tunable Coherent Parametric Oscillation in $LiNbO_3$ at Optical Frequencies," *Phys. Rev. Lett.* **14:**973–976 (1965).
3. R. L. Byer and A. Piskarskas, "Optical Parametric Oscillation and Amplification," Special Issue, *J. Opt. Soc. Am. B* **10:**1656–1791; 2148–2243 (1993).
4. W. R. Bosenberg and R. C. Eckardt, "Optical Parametric Devices," Special issue, *J. Opt. Soc. Am. B* **12:** 2084–2322 (1995).
5. S. Schiller and J. Mlynek, "Continuous-Wave Optical Parametric Oscillators," Special Issue, *Appl. Phys. B* **66:** 661–764 (1998).
6. M. Ebrahim-Zadeh, R. C. Eckardt, and M. H. Dunn, "Optical Parametric Devices and Processes," Special Issue, *J. Opt. Soc. Am. B* **16:**1477–1602 (1999).
7. M. Ebrahim-Zadeh, "Mid-Infrared Ultrafast and Continuous-Wave Optical Parametric Oscillators," in *Solid-State Mid-Infrared Laser Sources* (Springer, Berlin, Heidelberg, 2003) pp. 179–218.
8. M. Ebrahim-Zadeh, "Optical Parametric Devices," in *Handbook of Laser Technology and Applications* (Institute of Physics Publishing, London, 2003) pp. 1347–1392.
9. K. L. Vodopyanov, "Pulsed Mid-Infrared Optical Parametric Oscillators," in *Solid-State Mid-Infrared Laser Sources,* I. T. Sorokina and K. L. Vodopyanov, eds. (Springer, Berlin, Heidelberg, 2003) pp. 141–178.
10. M. Ebrahim-Zadeh, "Mid-Infrared Optical Parametric Oscillators and Applications," in *Mid-Infrared Coherent Sources and Applications*, M. Ebrahim-Zadeh and I. T. Sorokins, eds. (Springer, Berlin, Heidelberg, 2007) pp. 347–375.
11. R. L. Sutherland, *Handbook of Nonlinear Optics* (Marcel Dekker, New York, 1996).
12. M. H. Dunn and M. Ebrahim-Zadeh, "Parametric Generation of Tunable Light from Continuous-Wave to Femtosecond Pulses," *Science* **286:**1513–1517 (1999).
13. M. Ebrahim-Zadeh, "Parametric Light Generation," *Phil. Trans. Roy. Soc. London A* **263:**2731–2750 (2003).
14. S. E. Harris, "Tunable Optical Parametric Oscillators," *Proc. IEEE* **57:**2096–2113 (1969).

15. R. L. Byer, "Optical Parametric Oscillators," in *Treatise in Quantum Electronics* (Academic Press, New York, 1973) pp. 587–702.
16. R. G. Smith, "Optical Parametric Oscillators," in *Lasers* (Marcel Dekker, New York, 1976) pp. 189–307.
17. I. D. Lindsay, "High Spatial and Spectral Quality Diode-Laser-Based Pump Sources for Solid-State Lasers and Optical Parametric Oscillators," PhD. Thesis, University of St Andrews (1999).
18. T. J. Edwards, G. A. Turnbull, M. H. Dunn, and M. Ebrahim-Zadeh, "Continuous-Wave, Singly-Resonant, Optical Parametric Oscillator Based on Periodically Poled $KTiOPO_4$," *Opt. Exp.* **16:**58–63 (2000).
19. S. E. Bisson, K. M. Armstrong, T. J. Kulp, and M. Hartings, "Boradly Tunable, Mode-Hop-Tuned CW Optical Parametric Oscillator Based on Periodically Poled Lithium Niobate," *Appl. Phys. B* **40:**6049–6055 (2001).
20. M. Van Herpen, S. te Lintel Hekkert, S. E. Bisson, and F. J. M. Harren, "Wide Single-Mode Tuning of a 3.0–3.8-μm, 700-mW, Continuous-Wave Nd:YAG-Pumped Optical Parametric Oscillator Based on Periodically-Poled Lithium Niobate," *Opt. Lett.* **27:**640–642 (2002).
21. M. M. J. W. Van Herpen, S. Li, S. E. Bisson, S. te Lintel Hekkert, and F. J. M. Harren, "Tuning and Stability of Continuous-Wave Mid-Infrared High-Power Single Resonant Optical Parametric Oscillator," *Appl. Phys. B* **75:**329–333 (2002).
22. M. M. J. W. Van Herpen, S. E. Bisson, and F. J. M. Harren, "Continuous-Wave Operation of a Single-Frequency Optical Parametric Oscillator at 4–5 μm Based on Periodically Poled $LiNbO_3$," *Opt. Lett.* **28:**2497–2499 (2003).
23. M. M. J. W. Van Herpen, S. E. Bisson, A. K. Y. Ngai, and F. J. M. Harren, "Combined Wide Pump Tuning and High Power of a Continuous-Wave, Singly Resonant Optical Parametric Oscillator," *Appl. Phys. B* **78:**281–286 (2004).
24. A. K. Y. Ngai, S. T. Persijn, G. Von Basum, and F. J. M. Harren, "Automatically Tunable Continuous-Wave Optical Parametric Oscillator for High-Resolution Spectroscopy and Sensitive Trace-Gas Detection," *Appl. Phys. B* **85:**173–180 (2006).
25. P. Gross, M. E. Klein, T. Walde, K.-J. Boller, M. Auerbach, P. Wessels, and C. Fallnich, "Fiber-Laser-Pumped Continuous-Wave Singly Resonant Optical Parametric Oscillator," *Opt. Lett.* **27:**418–420 (2002).
26. M. E. Klein, P. Gross, K.-J. Boller, M. Auerbach, P. Wessels, and C. Fallnich, "Rapidly Tunable Continuous-Wave Optical Parametric Oscillator Pumped by a Fiber Laser," *Opt. Lett.* **28:**920–922 (2003).
27. A. Henderson and R. Stafford, "Low Threshold, Singly Resonant CW OPO Pumped by an All-Fiber Pump Source," *Opt. Exp.* **14:**767–772 (2006).
28. M. E. Klein, C. K. Laue, D.-H. Lee, K.-J. Boller, and R. Wallenstein, "Diode-Pumped Singly Resonant Continuous-Wave Optical Parametric Oscillator with Wide Continuous Tuning of the Near-Infrared Idler Wave," *Opt. Lett*. **25:**490–492 (2000).
29. I. D. Lindsay, B. Adhimoolam, P. Gross, M. E. Klein, and K.-J. Boller, "110 GHz Rapid, Continuous Tuning from an Optical Parametric Oscillator Pumped by a Fiber-Amplified DBR Diode Laser," *Opt. Exp.* **13:**1234–1239 (2005).
30. A. Henderson and R. Stafford, "Intracavity Power Effects in Singly Resonant CW OPOs," *Appl. Phys. B* **85:**181–184 (2006).
31. G. K. Samanta and M. Ebrahim-Zadeh, "Continuous-Wave Singly Resonant Optical Parametric Oscillator with Resonant Wave Coupling," *Opt. Exp.* **16:**6883–6888 (2008).
32. A. V. Okishev and J. D. Zuegel, "Intracavity-Pumped Raman Laser Action in a Mid-IR, Continuous-Wave (CW) MgO:PPLN Optical Parametric Oscillator", *Opt. Exp.* **14:**12169–12173 (2006).
33. A. Henderson and R. Stafford, "Spectral Broadening and Stimulated Raman Conversion in a Continuous-Wave Optical Parametric Oscillator," *Opt. Lett.* **32:**1281–1283 (2007).
34. U. Strossner, J. P. Meyn, R. Wallenstein, P. Urenski, A. Arie, G. Rosenman, J. Mlynek, S. Schiller, and A. Peters, "Single-Frequency Continuous-Wave Optical Parametric Oscillator System with an Ultrawide Tuning Range of 550–2830 nm," *J. Opt. Soc. Am. B* **19:**1419–1424 (2002).
35. G. K. Samanta, G. R. Fayaz, Z. Sun, and M. Ebrahim-Zadeh, "High-Power, Continuous-Wave, Singly Resonant Optical Parametric Oscillator Based on MgO:sPPLT," *Opt. Lett.* **32:**400–402 (2007).
36. G. K. Samanta, G. R. Fayaz, and M. Ebrahim-Zadeh, "1.59-W, Single-Frequency, Continuous-Wave Optical Parametric Oscillator Based on MgO:sPPLT," *Opt. Lett.* **32:**2623–2625 (2007).
37. J.-M. Melkonian, T.-H. My, F. Bretenaker, and C. Drag, "High Spectral Purity and Tunable Operation of a Continuous Singly Resonant Optical Parametric Oscillator Emitting in the Red," *Opt. Lett*. **32:**518–520 (2007).

38. G. K. Samanta and M. Ebrahim-Zadeh, "Continuous-Wave, Single-Frequency, Solid-State Blue Source for the 425-489 nm Spectral Range," *Opt. Lett.* **33:**1228–1230 (2008).
39. T.-H. My, C. Drag, and F. Bretenaker, "Single-Frequency and Tunable Operation of a Continuous Intracavity Frequency Doubled Singly Resonant Optical Parametric Oscillator," *Opt. Lett.* **33:**1455–1457 (2008).
40. C. Langrock and M. M. Fejer, "Fiber-Feedback Continuous-Wave and Synchronously Pumped Singly Resonant Ring Optical Parametric Oscillators Using Reverse-Proton-Exchanged Periodically Poled Lithium Niobate Waveguides," *Opt. Lett.* **32:**2263–2265 (2007).
41. A. J. Henderson, P. M. Roper, L. A. Borschowa, and R. D. Mead, "Stable, Continuously Tunable Operation of a Diode-Pumped Doubly Resonant Optical Parametric Oscillator," *Opt. Lett.* **25:**1264–1266 (2000).
42. T. Petelski, R. S. Conroy, K. Benecheikh, J. Mlynek, and S. Schiller, "All-Solid-State, Tunable, Single-Frequency Source of Yellow Light for High-Resolution Spectroscopy," *Opt. Lett.* **26:**1013–1015 (2001).
43. I. D. Lindsay, C. Petridis, M. H. Dunn, and M. Ebrahim-Zadeh, "Continuous-Wave Pump-Enhanced Singly Resonant Optical Parametric Oscillator Pumped by an Extended-Cavity Diode Laser," *Appl. Phys. Lett.* **78:**871–873 (2001).
44. G. A. Turnbull, D. McGloin, I. D. Lindsay, M. Ebrahim-Zadeh, and M. H. Dunn, "Extended Mode-Hop-Free Tuning by Use of Dual-Cavity, Pump-Enhanced Optical Parametric Oscillator," *Opt. Lett.* **25:**341–343 (2000).
45. D. J. M. Stothard, I. D. Lindsay, M. H. Dunn, "Continuous-Wave Pump-Enhanced Optical Parametric Oscillator with Ring Resonator for Wide and Continuous Tuning of Single-Frequency Radiation," *Opt. Exp.* **12:**502–511 (2004).
46. I. D. Lindsay, D. J. M. Stothard, C. F. Rae, and M. H. Dunn, "Continuous-Wave Pump-Enhanced Optical Parametric Oscillator Based on Periodically Poled $RbTiOAsO_4$," *Opt. Exp.* **11:**134–140 (2003).
47. F. Muller, G. Von Basum, A. Pop, D. Halmer, P. Hering, M. Murtz, F. Kunnermann, and S. Schiller, "Long-Term Frequency Stability and Linewidth Properties of Continuous-Wave Pump-Resonant Optical Parametric Oscillators," *Appl. Phys. B* **80:**307–313 (2005).
48. P. Gross, M. E. Klein, H. Ridderbusch, D.-H. Lee, J.-P. Meyn, R. Wallenstein, and K.-J. Boller, "Wide Wavelength Tuning of an Optical Parametric Oscillator Through Electro-Optic Shaping of the Gain Spectrum," *Opt. Lett.* **27:**1433–1435 (2002).
49. G. Ferrari, "Generating Green to Red Light with Semiconductor Lasers," *Opt. Exp.* **15:**1672–1678 (2007).
50. A. K. Y. Ngai, S. T. Persijn, I. D. Lindsay, A. A. Kosterev, P. Gross, C. J. Lee, S. M. Cristescu, F. K. Tittel, K.-J. Boller, and F. J. M. Harren, "Continuous Wave Optical Parametric Oscillator for Quartz-Enhanced Photoacoustic Trace Gas Sensing," *Appl. Phys. B* **89:**123–128 (2007).
51. E. V. Kovalchuk, D. Dekorsy, A. I. Lvovsky, C. Braxmaier, J. Mlynek, A. Peters, and S. Schiller, "High-Resolution Doppler-Free Molecular Spectroscopy with a Continuous-Wave Optical Parametric Oscillator," *Opt. Lett.* **26:**1430–1432 (2001).
52. F. Muller, A. Popp, F. Kuhnemann, and S. Schiller, "Transportable, Highly Sensitive Photoacoustic Spectrometer Based on Continuous-Wave Dual-Cavity Optical Parametric Oscillator," *Opt. Exp.* **11:**2820–2825 (2003).
53. G. von Basum, D. Halmer, P. Hering, M. Murtz, S. Schiller, F. Muller, A. Popp, and F. Kuhnemann, "Parts per Trillion Sensitivity for Ethane in Air with an Optical Parametric Oscillator Cavity Leak-Out Spectrometer," *Opt. Lett.* **29:**797–799 (2004).
54. D. J. M. Stothard, M. H. Dunn, and C. F. Rae, "Hyperspectral Imaging of Gases with a Continuous-Wave Pump-Enhanced Optical Parametric Oscillator," *Opt. Exp.* **12:**947–955 (2004).
55. K. Hayasaka, Y. Zhang, and K. Kasai, "Generation of Twin Beams from an Optical Parametric Oscillator Pumped by a Frequency-Doubled Diode Laser," *Opt. Lett.* **29:**1665–1667 (2004).
56. X. Su, A. Tan, X. Jia, Q Pan, C. Xie, and K. Peng, "Experimental Demonstration of Quantum Entanglement between Frequency Non-Degenerate Optical Twin Beams," *Opt. Lett.* **31:**1133–1135 (2006).
57. T. Tanimura, D. Akamatsu, Y. Yokoi, A. Furusawa, and M. Kozuma, "Generation of a Squeezed Vacuum Resonant on a Rubidium D_1 Line with Periodically Poled $KTiOPO_4$," *Opt. Lett.* **31:**2344–2364 (2006).
58. E. V. Kovalchuk, T. Schuldt, and A. Peters, "Combination of a Continuous-Wave Optical Parametric Oscillator and a Femtosecond Frequency Comb for Optical Frequency Metrology," *Opt. Lett.* **30:**3141–3143 (2005).